Received: 5 April 2019 | Revised: 29 July 2019 | Accepted: 5 August 2019

DOI: 10.1002/hbm.24767

WILEY

RESEARCH ARTICLE

Targeting age-related differences in brain and cognition with multimodal imaging and connectome topography profiling

Alexander J. Lowe[1] | Casey Paquola[1] | Reinder Vos de Wael[1] | Manesh Girn[2] | Sara Lariviere[1] | Shahin Tavakol[1] | Benoit Caldairou[3] | Jessica Royer[1] | Dewi V. Schrader[4] | Andrea Bernasconi[3] | Neda Bernasconi[3] | R. Nathan Spreng[2,5] | Boris C. Bernhardt[1]

[1]Multimodal Imaging and Connectome Analysis Laboratory, McConnell Brain Imaging Centre, Montreal Neurological Institute and Hospital, McGill University, Montreal, Canada

[2]Laboratory of Brain and Cognition, Montreal Neurological Institute, Department of Neurology and Neurosurgery, McGill University, Montreal, Canada

[3]Neuroimaging of Epilepsy Lab, McConnell Brain Imaging Centre, Montreal Neurological Institute and Hospital, McGill University, Montreal, Canada

[4]Department of Pediatrics, Faculty of Medicine, University of British Columbia, Vancouver, Canada

[5]Department of Psychiatry and Psychology, McGill University, Montreal, Canada

Correspondence
Boris C. Bernhardt, Multimodal Imaging and Connectome Analysis Lab, McConnell Brain Imaging Centre, Montreal Neurological Institute and Hospital, McGill University, Montreal, Quebec H3A 2B4, Canada.
Email: boris.bernhardt@mcgill.ca

Funding information
Canadian Institutes of Health Research, Grant/Award Number: Foundation

Abstract

Aging is characterized by accumulation of structural and metabolic changes in the brain. Recent studies suggest transmodal brain networks are especially sensitive to aging, which, we hypothesize, may be due to their apical position in the cortical hierarchy. Studying an open-access healthy cohort (n = 102, age range = 30–89 years) with MRI and Aβ PET data, we estimated age-related cortical thinning, hippocampal atrophy and Aβ deposition. In addition to carrying out surface-based morphological and metabolic mapping experiments, we stratified effects along neocortical and hippocampal resting-state functional connectome gradients derived from independent datasets. The cortical gradient depicts an axis of functional differentiation from sensory-motor regions to transmodal regions, whereas the hippocampal gradient recapitulates its long-axis. While age-related thinning and increased Aβ deposition occurred across the entire cortical topography, increased Aβ deposition was especially pronounced toward higher-order transmodal regions. Age-related atrophy was greater toward the posterior end of the hippocampal long-axis. No significant effect of age on Aβ deposition in the hippocampus was observed. Imaging markers correlated with behavioral measures of fluid intelligence and episodic memory in a topography-specific manner, confirmed using both univariate as well as multivariate analyses. Our results strengthen existing evidence of structural and metabolic change in the aging brain and support the use of connectivity gradients as a compact framework to analyze and conceptualize brain-based biomarkers of aging.

KEYWORDS
aging, amyloid, atrophy, cognition, hippocampus, neocortex

Alexander J. Lowe and Casey Paquola authors are contributed equally to this work.

1 | INTRODUCTION

Aging is a multifactorial process defined as a time-dependant functional decline that affects most living organisms (López-Otín, Blasco, Partridge, Serrano, & Kroemer, 2013). Though not fully understood, aging involves the accumulation of structural and metabolic changes that ultimately lead to impairments in multiple cognitive domains, including executive function, episodic memory, and word retrieval (Baciu et al., 2016; Fjell, Sneve, Grydeland, Storsve, & Walhovd, 2017; Tromp, Dufour, Lithfous, Pebayle, & Després, 2015). Collectively, these contribute to increasing challenges for psychosocial functioning, wellbeing, and quality of life in older age (Pan et al., 2015; Wilson et al., 2013).

Ongoing advances in multimodal neuroimaging have identified structural, functional, and metabolic substrates of both healthy cognitive functioning (Tomasi & Volkow, 2012) and of its decline in aging (Draganski, Lutti, & Kherif, 2013; McConathy & Sheline, 2015; Steffener, Brickman, Habeck, Salthouse, & Stern, 2013). In particular, progress in magnetic resonance imaging (MRI) acquisition and modeling techniques now allows for the fine-grained mapping of neocortical and subcortical morphology in vivo (Fischl & Dale, 2000). In healthy individuals, aging has been related to decreased hippocampal volume and cortical thinning (Fjell, McEvoy, Holland, Dale, & Walhovd, 2014; Fraser, Shaw, & Cherbuin, 2015; Salat et al., 2004; Shaw, Sachdev, Anstey, & Cherbuin, 2016; Sowell et al., 2003; Yang et al., 2016; Yao, Hu, Liang, Zhao, & Jackson, 2012), both of which measurably contribute to cognitive decline (Fjell et al., 2006; Leal & Yassa, 2015; Mielke et al., 2012; Walhovd et al., 2006). These findings are complemented by functional and metabolic studies, particularly work based on positron emission imaging (PET) of tracers sensitive to deposits associated with healthy and pathological aging. PET-based quantification of amyloid beta (Aβ), generally considered a marker of neurodegenerative conditions like Alzheimer's Disease, has demonstrated elevated levels in the brains of cognitively normal older adults as well (Jansen et al., 2015; Rodrigue et al., 2012; Sperling et al., 2011). Cortical Aβ has furthermore been associated with multi-domain cognitive impairment, such as episodic and semantic memory together with executive and visuospatial abilities (Baker et al., 2017; Farrell et al., 2017; Jansen et al., 2018; Mortamais et al., 2017).

With increasing availability of open-access and multimodal data aggregation and dissemination initiatives, it is now possible to adopt an integrated approach, combining several imaging markers to better understand biological factors contributing to cognitive decline. Recent studies in cognitively normal older adults have suggested a synergistic relationship between cerebral amyloid pathology and hippocampal atrophy (Bilgel et al., 2018), whereas others suggest that cortical thickness may represent a more approximate marker of the pathophysiological underpinning of cognitive decline than Aβ deposition (Knopman et al., 2018). In addition to the potentially complementary value of different imaging markers as surrogates of cognitive abilities, aging effects do not seem to be uniform across different regions (McGinnis, Brickhouse, Pascual, & Dickerson, 2011). Notably, several reports have supported an interaction between large-scale functional network organization, structural brain changes, and the risk for cognitive decline in aging (Andrews-Hanna et al., 2007; Buckner, 2004; Fox et al., 2005; Sambataro et al., 2010; Spreng, Wojtowicz, & Grady, 2010; Sullivan, Anderson, Turner, & Spreng, 2019; Spreng & Turner, 2013; Zhao et al., 2015). Structural and metabolic changes in transmodal regions known to engage in more higher-order and integrative processing, such as the default mode network (DMN) and fronto-parietal networks, have been demonstrated to contribute to cognitive decline in healthy subjects (Lim et al., 2014). An overlap between elements of the DMN and Aβ pathology has been previously reported in Alzheimer's Disease (Buckner, 2005), with recent studies indicating that core DMN regions may be among the earliest sites of Aβ deposition in preclinical stages (Palmqvist et al., 2017). This pathological accumulation is thought to contribute to memory dysfunction associated with dementia, as the DMN has been shown to be engaged during activation of episodic memory (Buckner, Andrews-Hanna, & Schacter, 2008). Pathological Aβ deposition is not unique to the DMN however, with early accumulation also reported in the fronto-parietal network as well as other transmodal regions with overall high long-range connectivity (Buckner et al., 2009; Elman et al., 2016; He et al., 2014; Wang et al., 2007).

Studying the openly-available Dallas Lifespan Aging Study (DLBS) dataset (Park, 2018), the current work integrated measures of neocortical and hippocampal morphology and Aβ deposition to examine age-related differences and their relationship to cognition. In addition to leveraging surface-based processing and multimodal co-registration techniques, we harnessed a novel analysis reference frame determined by the putative neocortical hierarchy. Initially formulated in nonhuman primates (Mesulam, 1998), the hierarchy follows a "sensory-fugal" gradient from low-level cortices involved in interactions with the external world to higher-order transmodal areas involved in self-generated, abstract cognition (Buckner & Krienen, 2013; Huntenburg, Bazin, & Margulies, 2018; Margulies et al., 2016; Paquola et al., 2019; Hong et al., 2019). Recent application of unsupervised compression techniques applied to cortico-cortical functional connectivity data recapitulated a similar gradient in humans (Margulies et al., 2016). By being functionally and anatomically distant from sensory systems, DMN activity is likely to be shielded from environmental input (Kiebel, Daunizeau, & Friston, 2008) and may also perform cross-modal integration of information (van den Heuvel & Sporns, 2013). Equivalent compression techniques have been applied to hippocampus-to-cortex connectivity profiles, also revealing a principal gradient of connectivity. In the hippocampus, this gradient follows its "long-axis," with anterior segments being closely connected to transmodal DMN and temporo-limbic networks, while posterior sections increasingly interact with posterior cortical areas including the visual and dorsal/ventral attention networks (Vos de Wael et al., 2018).

Stratification of aging biomarkers based on neocortical and hippocampal connectivity gradients, followed by univariate as well as multivariate analytics, provides an alternative viewpoint to voxel- or parcellation-based studies of macroscale organization and connectivity. This reference frame may help to consolidate recent literature

demonstrating increased vulnerability of higher-order networks to pathological protein accumulation (Buckner et al., 2009; Elman et al., 2016; He et al., 2014; Palmqvist et al., 2017), and age-related reductions in cortical thickness across higher-order and sensorimotor networks (Bajaj, Alkozei, Dailey, & Killgore, 2017). Furthermore, by sidestepping the need to define discrete communities through the use of clustering (Eickhoff, Yeo, & Genon, 2018; Yeo et al., 2011) or connectivity boundary mapping techniques (Cohen et al., 2008), gradient-based connectome profiling provides a continuous coordinate system to aggregate and analyze aging biomarkers. Ultimately, this approach allows for the multimodal study of pathological advance along a quantifiable map of the neocortical hierarchy and the hippocampal long-axis, furthering our understanding of neurological aging and the associated cognitive decline with respect to brain organization at the system level.

2 | MATERIALS AND METHODS

2.1 | Participants

We selected 144 healthy adult native English speakers (89 females, 30–89 years, mean ± SD age = 62 ± 16.9 years, 93.4% White/Caucasian) from the openly-shared DLBS, a comprehensive study designed to understand cognitive functioning at different stages of the adult lifespan (http://fcon_1000.projects.nitrc.org/indi/retro/dlbs.html; (Park, 2018). Participants were well educated (mean ± *SD* = 16.8 ± 2.3 years of education) and scored highly on the mini-mental state examination (MMSE; Folstein, Folstein, & McHugh, 1975; mean ± *SD* = 28 ± 1.2 points). As previously outlined (Rodrigue et al., 2012), participants were screened for neurological and psychiatric disorders, loss of consciousness >10 min from a traumatic insult to the head, drug/alcohol abuse, stroke and major heart surgery, chemotherapy within 5 years, and immune system disorders. Participants were right-handed and recruited from the Dallas–Fort Worth metropolitan area. Specifically, we selected only those who underwent a research-dedicated anatomical MRI and Aβ PET examination.

It is of note that all participants in the DLBS were classified as cognitively healthy as per MMSE scores. However, as the DLBS provides no measure of subjective cognitive decline (SCD), we were unable to exclude participants based on this variable, previously shown to relate to mesial temporal atrophy and functional connectivity alterations (Fan et al., 2018; Verfaillie et al., 2018). Additionally, clinical rating tools such as Scheltens visual rating of medial temporal atrophy scale (Scheltens, Launer, Barkhof, Weinstein, & van Gool, 1995) that can identify participants with preclinical Alzheimer's Disease, were not employed. Our dataset thus included physically healthy subjects with high MMSE scores indicative of intact cognition as supplied by DLBS, and without the additional exclusion of participants who may potentially have preclinical Alzheimer's Disease based on visual ratings.

The DLBS was approved by the University of Texas at Dallas and University of Texas Southwestern Medical Centre respective ethics committees. All DLBS participants provided written consent prior to enrolment.

2.2 | Neuropsychological test battery

Participants completed a battery of neuropsychological tests assessing the following domains; processing speed (Salthouse & Babcock, 1991; Wechsler, 2008), working memory (Turner & Engle, 1989; Wechsler, 2008), episodic memory (Brandt, 1991; Robbins et al., 2010), crystallized abilities (Zachary, 1986), executive function (Robbins et al., 2010), and fluid reasoning (Ekstrom, French, Harman, & Dermen, 1976; Raven, 1996). A single participant was missing a single score for the Digit Symbol Task (0.1% missing data). Due to this number being so small, we did not want to exclude the participant from analysis, but instead imputed the missing data point using linear interpolation. Results from all neuropsychological tests were standardized to *z*-scores. To reduce data dimensionality, we iteratively performed a maximum likelihood common factor analysis with varimax rotation with two- to five-factor solutions (Harman, 1976). Overfitting occurred with three or more factors (Heywood, 1931), thus the two-factor solution was utilized in subsequent analyses. Neuropsychological tests pertaining to fluid intelligence strongly contributed to the first factor (*henceforth*, F1), specifically Ravens Progressive matrices, Educational Testing Service (ETS) Letter Sets, Digit Symbol Test, Digit Comparison Test, CANTAB Spatial Working Memory Test, and CANTAB Stockings of Cambridge Test. Whereas tests pertaining to episodic memory contributed highly to the second factor 2 (F2), specifically Hopkins Verbal Learning Immediate Recall, Delayed Recall, and Recognition. For specific factor loadings across tests, see Table S1.

2.3 | MRI acquisition

Anatomical images were acquired with a Philips Achieva 3 T whole-body scanner (Philips Medical Systems, Bothell, WA) and a Philips eight-channel head coil at the University of Texas Southwestern Medical Center using the Philips SENSE parallel acquisition technique. A 3D T1-weighted sagittal magnetization-prepared rapid acquisition gradient echo (MPRAGE) structural image was obtained (T1w, Repetition time [TR] = 8.1 ms, echo time [TE] = 3.7 ms, flip-angle = 12°, FOV = 204×256 mm^2, resulting in 160 slices with $1 \times 1 \times 1$ mm^3 voxels).

2.4 | Amyloid PET acquisition

All participants were injected with a 370 MBq (10 mCi) bolus of ^{18}F-Florbetapir. At 30 min post-injection, they were positioned on the imaging table of a Siemens ECAT HR PET scanner. Velcro straps and foam wedges were used to secure the participants head and participant positioning was completed using laser guides. A 2-min scout was acquired to ensure the brain was in the field of view and that there was no rotation in either plane. At 50 min post-injection, a two-frame by 5-min dynamic emission acquisition was started, followed

immediately by a 7-min internal rod source transmission scan. The transmission image was reconstructed using backprojection and a 6-mm full-width-at-half-maximum (FWHM) Gaussian filter. Emission images were processed by iterative reconstruction, specifically 4 iterations and 16 subsets with a 3 mm FWHM ramp filter.

2.5 | Multimodal image processing in neocortical and hippocampal regions

2.5.1 | Generation of neocortical surfaces

To generate models of the cortical surface and measure cortical thickness, native T1w images of each participant were processed using FreeSurfer 6.0 (http://surfer.nmr.mgh.harvard.edu). Previous work has cross-validated this pipeline with histological analysis (Cardinale et al., 2014; Rosas et al., 2002) and manual measurements (Kuperberg et al., 2003). Processing steps have been described in detail elsewhere (Dale, Fischl, & Sereno, 1999; Fischl, Sereno, & Dale, 1999). In short, the pipeline includes brain extraction, tissue segmentation, pial and white matter surface generation, and registration of individual cortical surfaces to the fsaverage surface template. The latter step aligns vertices among participants, while minimizing metric distortion. Cortical thickness was calculated as the closest distance from the white matter to the pial boundary at each vertex. FreeSurfer quality control and manual edits were carried out by a single rater (AL) and included pial corrections and addition of control points, followed by reprocessing.

2.5.2 | Hippocampal subfield-surface mapping

We applied a recently developed approach for hippocampal subfield segmentation, the generation of surfaces running through the core of each subfield, and subsequent "unfolding" for surface-based analysis of hippocampal imaging features (Bernhardt et al., 2016; Caldairou et al., 2016; Kim et al., 2014; Vos de Wael et al., 2018). In brief, each participant's native-space T1w image underwent automated correction for intensity nonuniformity, intensity standardization, and linear registration to the MNI152 template. Each image was processed using a multi-template surface-patch algorithm (Caldairou et al., 2016), which automatically segments the hippocampal formation into subiculum, CA1-3, and CA4-DG subfields. An open-access database of manual subfield segmentations and corresponding high-resolution 3 T MRI data (Kulaga-Yoskovitz et al., 2015) was used to train the algorithm (https://www.nitrc.org/projects/mni-hisub25). The algorithm was previously validated in healthy individuals, where Dice coefficients above 0.8 were demonstrated across subfields even when millimetric T1w images were used as input (Caldairou et al., 2016). The algorithm also generates medial sheet representations running through the core of each subfield, which allow for the sampling of intensity parameters with minimal partial volume effect, while guaranteeing point correspondence across participants. Prior validation experiments in epileptic patients showed that these features reliably predict hippocampal histopathology and focus laterality (Bernhardt et al., 2016, 2017; Kim et al., 2014). After parametrizing subfield surfaces using spherical harmonic shape descriptors (Styner et al., 2006), a Hamilton-Jacobi approach generated a medial surface running through the central path of each subfield (Kim et al., 2014). To estimate local atrophy, we calculated columnar volume (Kim et al., 2014). This index is calculated as the distance between a vertex on the medial sheet of each subfield and the corresponding outer shell multiplied by the average surface area of the surrounding triangles between the subfield boundary and the medial surface. In prior work, we showed a high correlation between columnar volume and degrees of hippocampal cell loss in patients with temporal lobe epilepsy (Bernhardt et al., 2016).

2.5.3 | PET-MRI integration

We mapped PET data to T1w imaging space generated by the pipelines in Section 2.5.1 and Section 2.5.2, allowing for a surface-based integration of Aβ uptake with structural imaging features along neocortical and hippocampal subfield surfaces. In both cases, boundary-based procedures estimated the registration between a native PET image and the corresponding T1w images (Greve & Fischl, 2009), followed by vertex-wise interpolation within the cortical ribbon. Neocortical PET data were resampled to fsaverage5 to improve correspondence across measurements; in the case of hippocampal PET features, the sampling grid was already aligned via the spherical parameterization during processing (Kim et al., 2014). Following previous approaches (Rodrigue et al., 2012), neocortical and hippocampal Aβ values were normalized by mean cerebellar gray matter Aβ uptake, providing a standardized uptake value ratio (SUVR) per vertex. To control for cerebro-spinal fluid partial volume effects (CSF-PVE), each participant's T1w image was skull stripped and segmented into tissue types and partial volume estimates (Zhang, Brady, & Smith, 2001). CSF-PVE maps were mapped to neocortical and hippocampal surfaces. Using surface-wide linear models, we controlled Aβ SUVR values for effects of CSF-PVE at each vertex in all participants (see Figure S1 for surface maps normalized by cerebellar gray matter only).

2.6 | Quality control and final sample selection

The DLBS open-access data set contains structural and functional data with variable image quality. All T1w images, segmentations, and co-registrations were visually inspected by a single researcher (AL). We removed datasets with artifacts leading to inaccurate cortical segmentations (n = 25) Additionally, data with inaccurate hippocampal segmentations (n = 17), characterized by gross errors or inclusion of neighboring white matter voxels, were removed. Following quality control, the final sample included 102 healthy individuals (69 females, 30–89 years, mean ± SD age = 59 ± 16.1 years, 90.2% White/Caucasian), who were highly educated (mean ± SD = 16.1 ± 2.2 years of education), and scored highly on the MMSE (mean ± SD = 28 ± 1.1). The age of our sample was approximately normally distributed (Figure S2).

2.7 | Statistical analysis

Analyses were performed using SurfStat (Worsley et al., 2009) for Matlab (The Mathworks, Natick, MA, R2017B). All linear models outlined below additionally controlled for sex and years of education.

2.7.1 | Regional analysis along neocortical and hippocampal surfaces

Surface-wide linear models examined effects of age on cortical thickness.

$$T_i = \beta_0 + \beta_1 * Age + \beta_2 * Sex + \beta_3 * Education$$

Where T_i is the thickness at vertex *i*, and *Age*, *Sex*, and *Education* are the model terms and the *betas* the estimated model parameters. Similar models assessed the relationship between cortical Aβ deposition and age. We corrected for multiple comparisons using the false discovery rate (FDR) procedure (Benjamini & Hochberg, 1995). We selected a two-tailed p_{FDR} of <.05. An analogous approach assessed age effects on columnar volume and Aβ across hippocampal subfield surfaces.

2.7.2 | Relation to cognitive factors

We computed Pearson's correlation coefficients and tested for associations between age and neuropsychological factor scores F1 and F2. Furthermore, we correlated mean cortical thickness, hippocampal volume, and Aβ values within significant clusters computed in Section 2.7.1 with the factor scores. As for the previous analysis, findings were corrected using an FDR procedure.

2.7.3 | Multimodal profiling based on connectome topographic mapping

We used previously derived maps of neocortical and hippocampal resting-state functional connectome gradients (Margulies et al., 2016; Vos de Wael et al., 2018) based on the human connectome project dataset (Van Essen et al., 2012) to stratify findings. In the neocortex, the first principal gradient describes a continuous transition from unimodal sensory areas via task-positive networks, such as the salience, dorsal attention, and fronto-parietal network, toward the DMN core regions (Margulies et al., 2016), recapitulating earlier models of a cortical hierarchy with low-level sensorimotor regions on the one end, and transmodal regions participating in higher-order functions on the other end (Mesulam, 1998). In the hippocampus, the first principal gradient of hippocampal connectivity runs from anterior to posterior regions across all subfields, with the former being more strongly connected to transmodal DMN than the posterior part (Vos de Wael et al., 2018). Both gradients were discretized into 20 bins, following a recent approach to stratify task-based fMRI data using connectome topographies (Murphy et al., 2018). In brief, depending on its location on the original gradient map, each voxel was assigned a label between 0 and 100, where 0 represents the unimodal end and 100 the transmodal end. Voxels were then assigned to a bin depending on their numerical label, for example, all voxels with a value between 0 and 5 were assigned to Bin 1 etc. Each bin contained the same number of vertices to ensure comparable sensitivity. We employed the same analysis as in Section 2.7.1 and mapped significant *t*-values to the discretized gradient using a sliding window approach. For all participants, the *t*-statistic for each voxel was calculated and averaged to produce a single *t*-value, which was assigned to the appropriate bin. Thus, each gradient bin had a specific *t*-value representing the average effect of age on brain markers in that bin. A linear model between bin ordering and the *t*-value within each bin explored interactions between gradient ordering and age effects on brain markers. To assess the relationship between gradient values and cognition, we computed the mean cortical thickness and amyloid values in each of the 20 gradient bins controlling for gender and level of education. The residual bin values were then fed into a linear model with factor Score 1 and 2 and resultant *t*-values were plotted against bin ordering to produce gradient-cognition plots. A linear model between bin ordering and the *t*-values then explored interaction between gradient ordering and cognition. This approach, thus, provided a low-dimensional representation of structural and Aβ changes along the neocortical and hippocampal functional topography.

2.7.4 | Additional control analyses

Replicability of the brain-cognitive relationships were assessed using complementary multivariate methods, specifically partial least squares (PLS) analysis (McIntosh & Lobaugh, 2004). PLS seeks to find weighted linear combinations of the original variables that maximally covary with each other. The PLS was optimized were surface-based brain measures (atrophy and Aβ scores; *z*-scored and arranged in matrix X) and cognitive and demographic phenotypes (*z*-scored and arranged in matrix; Y). Statistical significance of each latent variable was established via permutation tests, in which the rows of X were randomly permuted. For a given significant latent variable, we furthermore computed bootstrap ratios and their confidence intervals for each of the loadings, both for brain and phenotypic measures. To assess generalizability, we assessed the range of correlation coefficients when using a fivefold cross-validation paradigm.

3 | RESULTS

3.1 | Effects of age on neocortical and hippocampal subfield markers

3.1.1 | Surface-based findings

Vertex-wise analysis revealed widespread reductions in cortical thickness with increasing age (p_{FDR} < .025; Figure 1a). Laterally, clusters occupied bilateral frontal, central, temporal, and parietal cortices with a relative sparing of the orbitofrontal and occipital cortices. Medially, clusters occupied bilateral precuneus, cingulate, paracentral, superior frontal, fusiform, and parahippocampal cortices. Considering the hippocampus, subfield analysis of columnar volume revealed effects predominantly in posterior portions, spanning subiculum, CA1-3, and CA4-DG bilaterally. Additional clusters were also observed in bilateral anterior CA1-3 (p_{FDR} < .025; Figure 1a).

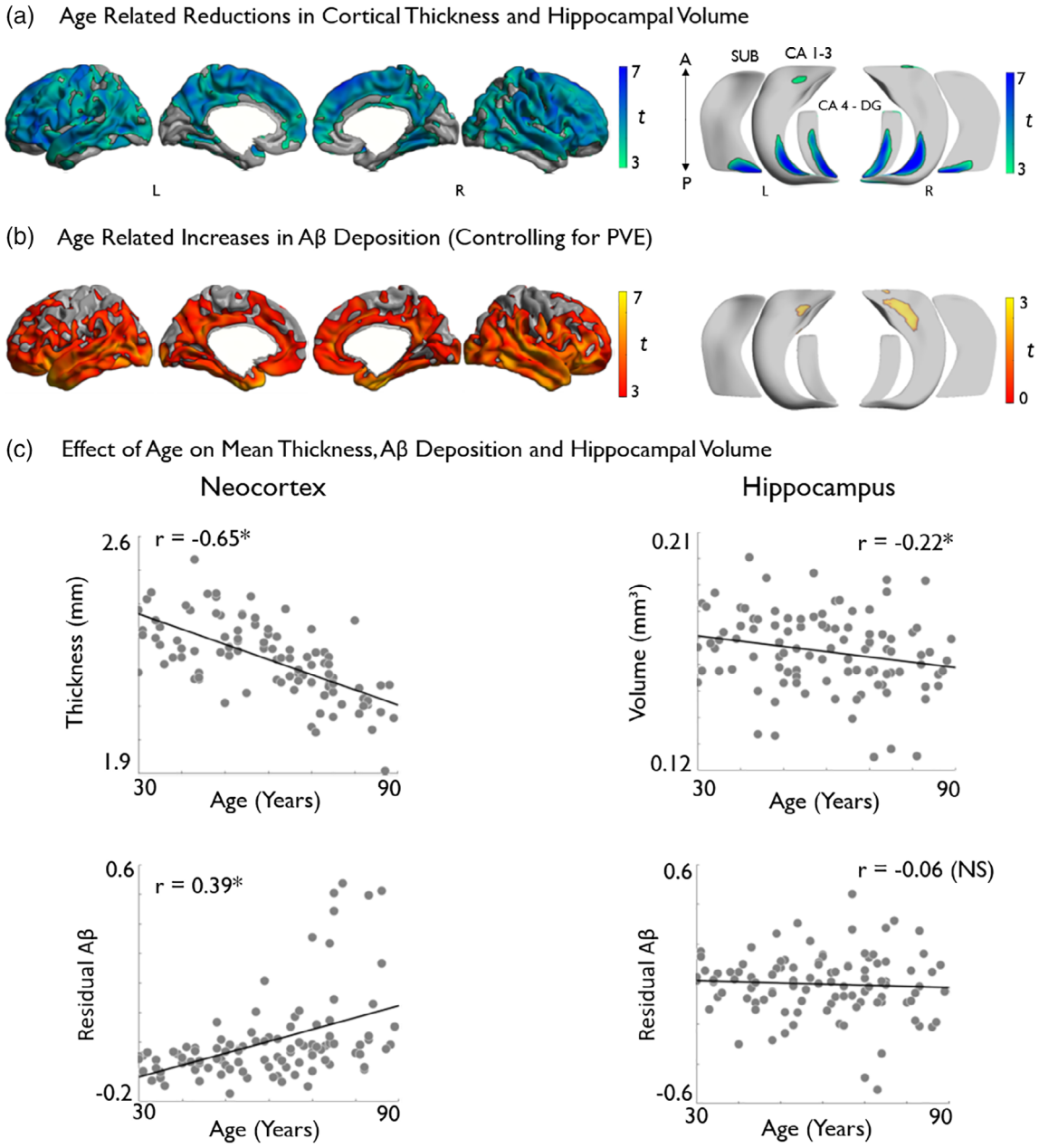

FIGURE 1 Analysis of gray matter morphology and Aβ deposition (normalized by cerebellar gray matter and controlled for CSF-PVE) along neocortical (*left*) and hippocampal subfield (*right*) surfaces. Effects of age on (a) cortical thickness and hippocampal volume across all subfields and (b) on Aβ deposition. Models controlled for sex and education. Age-related increases are shown in warm and decreases in cold colors. Regions significant at a two-tailed $p_{FDR} < .05$ are shown with black outlines, uncorrected trends relating to increased hippocampal Aβ are shown in semi-transparent (b, *bottom right*). Correlations between age and markers of brain aging are displayed in (c). *Denotes statistical significance. NS, nonsignificant; PVE, partial volume effect [Color figure can be viewed at wileyonlinelibrary.com]

We observed higher Aβ deposition with increasing age ($p_{FDR} < .025$) in a different spatial pattern than the cortical thickness findings. Specifically, we observed bilateral increases in predominantly limbic and transmodal cortices, encompassing lateral and medial temporal, insula, orbitofrontal, cingulate and midline parietal, as well as supramarginal regions, with a relative sparing of primary motor, occipital and mesial frontal cortices (Figure 1b). In the hippocampus, neither increases nor decreases in Aβ survived FDR-correction. At uncorrected thresholds ($p < .025$), we observed mainly trends for increased Aβ in bilateral anterior CA1-3 (Figure 1b).

Please see Figure S3 for more conservative surface-based effects thresholded at $p_{FDR} < .0001$.

3.1.2 | Mean neocortical and hippocampal effects

Pearson's correlations explore the relationship between age and overall neocortical and hippocampal brain markers. Analysis revealed both cortical thickness ($r = -.65$, $p < .01$) and hippocampal volume ($r = -.22$, $p < .05$) to display significant negative associations with age

(Figure 1c). A significant positive association was observed between age and cortical Aβ deposition (r = .39, p < .01). Unlike the neocortical findings, hippocampal Aβ deposition did not correlate with age (Figure 1c).

3.2 | Effects of age and imaging markers on cognition

Older age correlated with lower cognitive factors scores that is, poorer fluid intelligence (F1: r = −.66, p < .001) and episodic memory (F2: r = −.48, p < .001; Figure 2a).

Posthoc analysis between mean cortical thickness in regions of significant age effects (see Figure 1a) showed positive correlations with both F1 (r = .58, p < .001) and F2 (r = .41, p < .001), indicating better performance in individuals with higher thickness (Figure 2b). On the other hand, increases in mean Aβ deposition (see Figure 1b) related to lower scores on both F1 (r = −.31, p < .001) and F2 (r = −.23, p < .05; Figure 2b). At the level of the hippocampus, we observed positive correlations between columnar volumes in regions of age effects and F1 (r = .55, p < .001) and F2 (r = .43, p < .001). Regarding hippocampal Aβ deposition in regions of uncorrected age effects, no significant correlations were observed with F1 (r = −.15, p = .13) nor with F2 (r = −.08, p = .3).

In keeping with our study focus on aging rather than inter-individual differences, we opted not to control for age when assessing the relationship brain markers and cognition. We hypothesized that change in brain structure, Aβ deposition and age are related, and serve to impact on cognition in a synergistic manner. Therefore, a posthoc mediation analysis between age, cognition, and brain markers in regions of significant age effects was performed to explore this interdependence. The brain markers selected as potential mediators were those which demonstrated a significant correlation with both factor scores (Figure 2b,c). As such, hippocampal Aβ deposition was not included. Following the methodology described by Zhao, Lynch, and Chen (2010), we found cortical thickness (F1: $a*b$ = 0.007 [CI = 0.005–0.009], F2: $a*b$ = 0.004 [CI = 0.003–0.006]) cortical Aβ deposition (F1: $a*b$ = −0.002 [CI = −0.004 - -0.002], F2: $a*b$ = −0.001 [CI = −0.003 - 0.000]) and hippocampal volume (F1: $a*b$ = 0.006 [CI = 0.005–0.008]. F2: $a*b$ = 0.005 [CI = 0.003–0.006]) all to be significant mediators of the relationship between age and both F1 and F2. All brain markers were categorized as "Complimentary" mediators (Zhao et al., 2010), indicating the likely presence of additional mediating variables on the relationship between age and cognition.

3.3 | Profiling of age effects on brain markers and cognition via connectome gradients

3.3.1 | Age effects

Age-related cortical thinning was diffuse across the entire cortical functional gradient (p_{FDR} < .025), with no marked difference between uni- and transmodal areas (t = −1.64, p = .11; Figure 3a). On the other hand, although age-related increases in Aβ deposition also occurred across the entire neocortical gradient, we observed a significant incline toward transmodal regions (t = 6.96, p < .001; Figure 3a). Hippocampal age effects were not as strong as in the neocortex and did not reach significance. Yet, effect sizes for age-related volume loss were larger toward the posterior aspect of the hippocampal "long-axis" gradient (t = −9.51, p < .001) while we observed trends for increased Aβ in anterior regions (Figure 3b).

3.3.2 | Laminar differentiation

We also mapped levels of laminar differentiation to our cortical surface models similar to our previous work integrating 3D histology and neuroimaging (Paquola et al., 2019; Figure 3a). To this end, each cortical node was assigned to one of four levels of laminar differentiation (i.e., idiotypic, unimodal, heteromodal, paralimbic) derived from a seminal model of the cortical hierarchy based on the integration of neuroanatomical, electrophysiological, and behavioral studies in human and nonhuman primates (Mesulam, 1998). Laminar differentiation-based analysis confirmed highest aging related Aβ deposition in limbic transmodal areas (t > 3.9), and effect sizes descending the hierarchy that is, heteromodal association areas and unimodal association areas (t = 3.5) followed by idiotypic sensory and motor cortices (t = 2.77). For thickness findings, effects were more diffuse with highest negative aging effects in unimodal and heteromodal association areas (t > 3.3), followed by idiotypic (t = 3.0), and then limbic areas (t = 2.0; Figure 3a).

3.3.3 | Cognition

Considering cortical thickness, measures across the entire neocortical gradient positively correlated with F1, with largest effects in sensory regions (t = −2.40, p < .05), and with F2, which demonstrated no significant difference between sensory and higher-order bins (t = −1.60, p = .13). Aβ deposition across almost the entire gradient correlated with F1. In contrast to the thickness findings, transmodal values were most closely related to F1 scores (t = −5.00, p < .001). On the contrary, gradient-wise Aβ deposition showed no association with F2 scores (Figure 3c).

Hippocampal volume in low-level bins, corresponding to the posterior hippocampus correlated with higher F1 (t = −16.33, p < .001; Figure 3c) and F2 scores. Values in the posterior aspect of the gradient showed stronger correlations than those in anterior portions (t = −15.44, p < .001). Unlike the neocortical findings, gradient-wise hippocampal Aβ deposition did not correlate with scores for F1 and F2 (Figure 3c).

3.4 | Additional control analyses

Although main models included sex and education as control covariates, similar effects were observed using models that omitted their control (Figure S4). Furthermore, we observed virtually identical results when additionally controlling for APOE-e4 genotype (Figure S5), and when performing a subgroup analysis restricted to only non-APOE4-e4 carriers (Figure S6).

Univariate methods, as presented above, help to spatially pinpoint brain-cognition relationships (McIntosh & Lobaugh, 2010), and owing to their clear interpretability, lend themselves to integration with

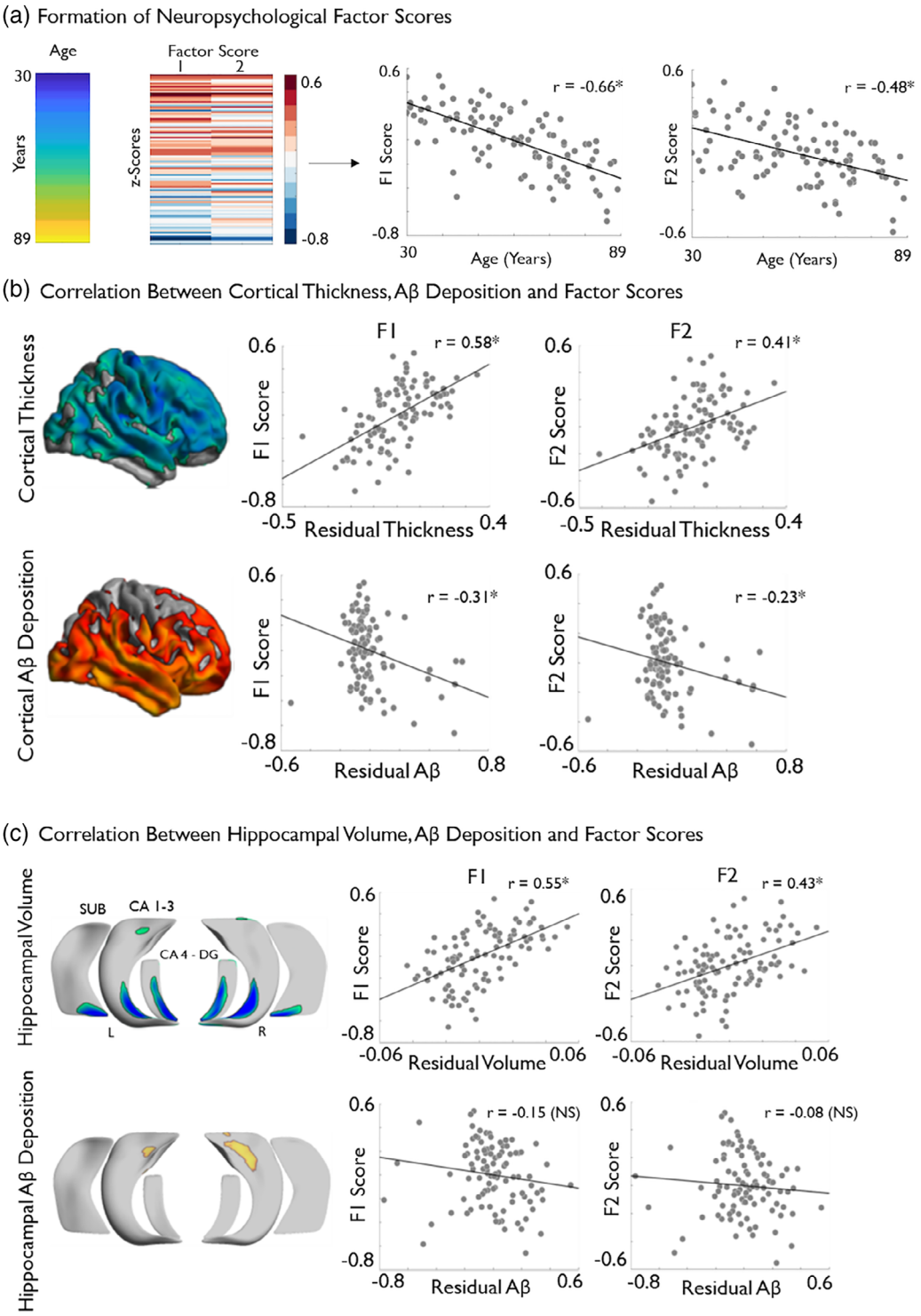

FIGURE 2 Associations between age-related brain markers and cognitive performance. (a) Age of sample is displayed next to the results of the maximum likelihood common factor analysis with varimax rotation, which identified two latent factors pertaining to measures of fluid intelligence (F1) and episodic memory (F2), respectively. The factor score matrix has been age-ordered with red indicating higher scores and blue indicated lower scores. Significant negative correlations between age and F1 and F2 scores are also displayed. (b) *Posthoc* correlation analysis, based on significant clusters of age-related cortical thickness and cortical amyloid deposition (see Figure 1) with F1 and F2. (c) Correlation analysis between hippocampal volume and amyloid deposition with F1 and F2. Brain measures have been corrected for sex and education. Please see Figure 1 for details on the multiple comparison's correction. *Denotes statistical significance. NS, nonsignificant; SUVR, standardized uptake value ratio [Color figure can be viewed at wileyonlinelibrary.com]

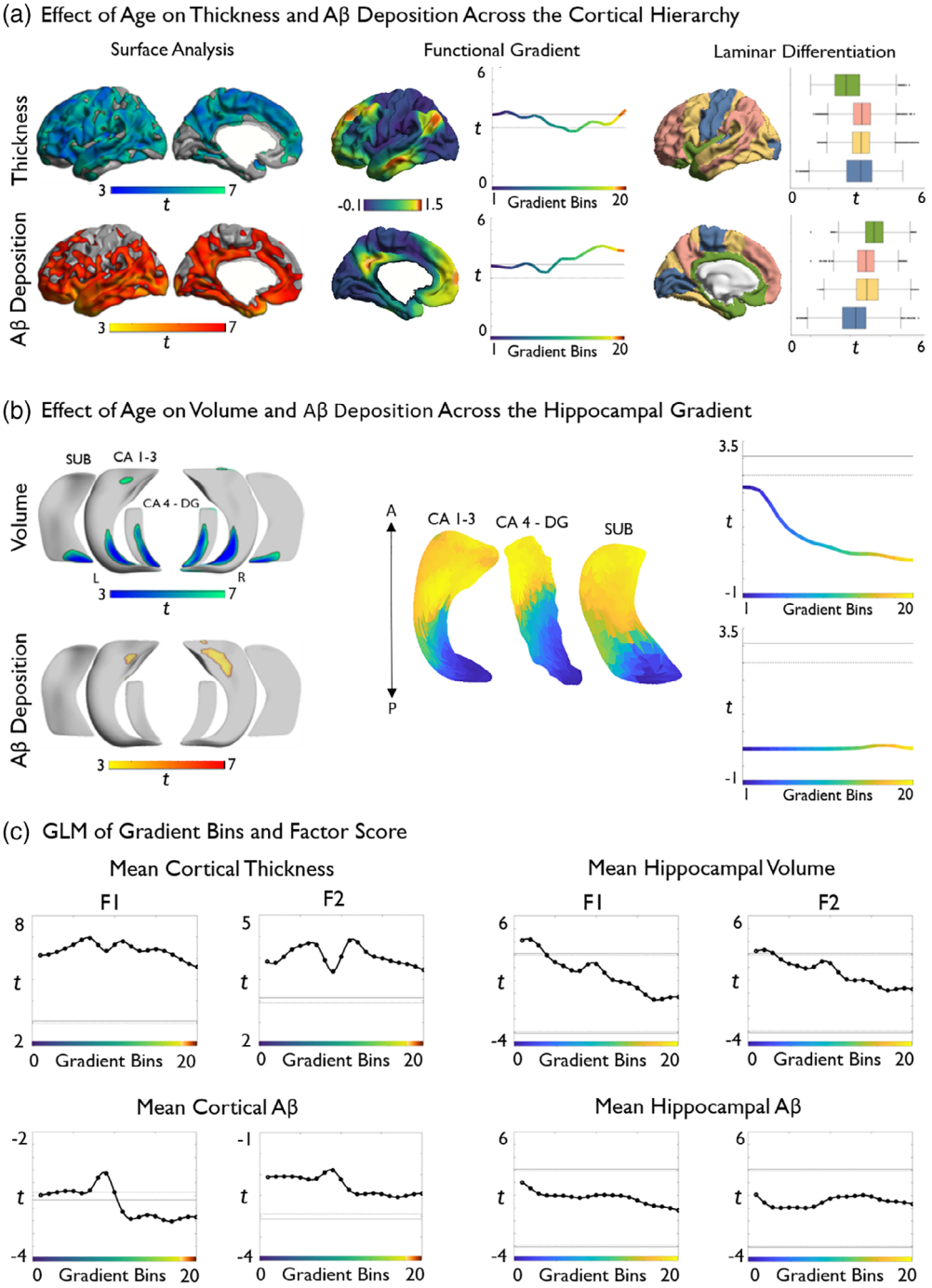

FIGURE 3 Topographic profiling of age effects and cognitive correlations in neocortical and hippocampal regions. (a) Age effects on vertex-wise cortical thickness and Aβ deposition (*left*), mapped to a reference space based on neocortical functional connectivity gradients (*center*, adapted from Margulies et al., 2016), resulting in a continuous profile of thickness values that can be correlated with age (*right*). In the profile, primary sensory regions are situated toward the left and transmodal regions toward the right. Profiles show consistently high aging effects on cortical thickness across the entire neocortical gradient. Aβ shows a similar pattern, but higher values toward the transmodal end. (b) Vertex-wise age effects on hippocampal subregional volume and Aβ deposition (*left*), mapped to a "long-axis" reference space based on hippocampal functional connectivity gradients (*center*, adapted from Vos de Wael et al., 2018), showing more elevated deposition in anterior subregions. Right hemisphere gradients were virtually identical. (c) Gradient-based stratification of correlations between F1 and F2 on neocortical *(left panels)* and hippocampal measures *(right panels)*. Solid lines represent significant *t*-values using Bonferroni correction, whereas dashed lines represent significant t-values using FDR-correction for multiple comparisons *(one-tailed $p < .025$)*. If the curve is above the positive lines, then brain marker values within that given bin significantly predict a higher cognitive score. Likewise, if the curve is below the negative lines then this is predictive of lower cognitive scores. If the curve falls between positive and negative lines, no statistical significance was achieved [Color figure can be viewed at wileyonlinelibrary.com]

second-level analysis, such as topographic profiling. We also performed PLS to synoptically interrogate brain-cognition relationships in a multivariate manner (Abdi & Williams, 2010; McIntosh & Mišić, 2013; Wold, 1966; Zeighami et al., 2017). The first demographic/cognitive latent variable was consistently characterized by aging and multi-domain cognitive impairment (Figure S7). On the other hand, we found robust and significant latent brain variables in three of the four models. At the level of the neocortex, this latent variable was associated with diffuse cortical atrophy (mean ± *SD r* across 100 fivefolds = 0.68 ± 0.09; permutation-test $p < .001$) and transmodal/paralimbic amyloid beta increases (mean ± *SD r* across 100 fivefolds = 0.40 ± 0.14; permutation-test $p = .003$). At the level of the hippocampus, the most significant latent variable was mainly characterized by subfield atrophy in posterior regions (mean ± *SD r* across 100 fivefolds = 0.67 ± 0.09, permutation-test $p < .001$), however hippocampal amyloid changes were not consistently related to the aging and cognitive impairment latent variable (mean ± *SD r* across 100 fivefolds = −0.05 ± 0.20, permutation-test $p = .298$).

Given that functional connectivity in healthy individuals has been shown to differ with age (Ferreira et al., 2016; Sala-Llonch et al., 2014), we also performed a separate control analysis in which we built functional connectivity gradients in the hippocampus and neocortex from a different healthy life span dataset ($n = 39$, 20 females, age range: 18–77, mean ± *SD* = 45 ± 22.9 years; Supporting Information "Methods"). Gradients estimated in this cohort were largely similar in overall shape to the original ones that is, describing a system level transition from unimodal to transmodal areas in neocortices and the hippocampal long-axis. Gradient-stratified findings based on the lifespan functional data were thus virtually identical to the original findings based on the HCP cohort, both for the neocortex (Figure S8) and hippocampus (Figure S9).

4 | DISCUSSION

Our work targeted age-related differences in morphology and amyloid deposition across neocortical and hippocampal subregions and confirms widespread structural-metabolic differences with advancing age. Age effects on thickness were diffuse along the entire neocortical functional gradient, whereas effects on volume were stronger in posterior segments of the hippocampal long-axis. Regarding Aβ deposition, age-related increases were observed along the entire neocortical gradient with significantly stronger effects observed in higher-order transmodal neocortices while no gradient-based modulation of age effects was observed for hippocampal Aβ. Structural and amyloid measures correlated with behavioral indices of fluid intelligence and episodic memory, again in a topography-dependent manner, emphasizing the power of our analytical framework to compactly represent and conceptualize brain aging in the context of macroscale functional systems.

At a whole-brain level, our image processing strategy incorporated several desirable elements to combine imaging metrics of neocortical and hippocampal subregions. Indeed, unconstrained surface-based morphometric MRI and Aβ PET analysis in neocortical regions extends work focusing on a-priori defined region-of-interest (Rodrigue et al., 2012; Thambisetty et al., 2010). Likewise, we deemed it essential to leverage a novel hippocampal segmentation algorithm due to the heterogenous nature of the structure. This heterogeneity extends along its anterior–posterior axis, across its three subregions and is characterized by differences in volume, functional connectivity, and vulnerability to aging and disease (Hatanpaa et al., 2014; Malykhin, Huang, Hrybouski, & Olsen, 2017; Poppenk, Evensmoen, Moscovitch, & Nadel, 2013; Vos de Wael et al., 2018). By unfolding its complex and interlocked anatomical organization, we could thus address subregional changes in the hippocampal formation along its long-axis, building upon prior work operating at the whole-hippocampus (Fjell et al., 2009) or whole-subfield level (de Flores, La Joie, & Chételat, 2015). Notably, although Aβ sampling was carried out within the cortical ribbon to minimize cerebro-spinal fluid partial voluming, we additionally controlled for these effects at each vertex using statistical techniques and normalized Aβ uptake data against cerebellar gray matter values, a reference region thought to be relatively unaffected by aging (Rodrigue et al., 2012; Vandenberghe et al., 2010). These steps likely increased specificity, while minimizing morphological confounds. At the level of the neocortical surface, we could observe a divergence between the effects of age on thickness and Aβ. Indeed, while the former affected a widespread network encompassing frontal, temporal and central areas in line with prior work (Fjell et al., 2009; McGinnis et al., 2011; Salat et al., 2004; Yang et al., 2016; Yao et al., 2012), increased Aβ was observed in a more restrictive and predominantly limbic transmodal circuitry (Rodrigue et al., 2012; Sperling et al., 2009). Following FreeSurfer edits and quality control, results remained largely the same, supporting that little or no age-related differences reflect a genuine sparing with increasing age. The regional divergence of morphological and Aβ effects was paralleled in the hippocampus, where we observed age-related reductions in local columnar volume mainly in posterior segments, while Aβ was marginally increased in the proximity of the hippocampal head.

To conceptualize these spatial patterns in a framework that more closely relates to macroscale functional organization, we utilized novel topographic mapping techniques guided by resting-state functional connectivity information from a large sample of healthy adults. Specifically, we remapped cortical and hippocampal morphometric and Aβ measures according to the main axes of neocortical and hippocampal connectivity. Prior work has shown that neocortical connectivity variations follow a gradient running from unimodal toward transmodal regions while hippocampal connectivity gradually shifts along its long-axis (Hong et al., 2019; Margulies et al., 2016; Plachti et al., 2019; Vos de Wael et al., 2018). Representing neuroimaging data in this compact, and presumably hierarchical (Mesulam, 1998), reference frame can be seen as complementary to parcellation-based methods as it does not assume clear-cut boundaries between functional systems but rather gradual transitions when going from one network to the next. In keeping with our regional findings, topography-stratified analysis supported a difference between structural and Aβ changes relative to the neocortical axes. While age effects on thickness were seen along the entire gradient, positive age-Aβ correlations were

significantly larger toward the transmodal anchor. Our findings with respect to functional connectivity gradients is compatible with earlier work demonstrating age-related cortical thinning across multiple functional networks (Bajaj et al., 2017), and a selective vulnerability of higher-order midline networks to Aβ pathology (Mutlu et al., 2017; Myers et al., 2014; Palmqvist et al., 2017; Rapoport, 1989; Sperling et al., 2009). From a theoretical perspective, our approach complements earlier models assuming a spatial patterning of brain aging, for example, models presuming that posterior structural and associated functional compromise may lead to increased activity in anterior regions (Davis, Dennis, Daselaar, Fleck, & Cabeza, 2008; Grady et al., 1994; Payer et al., 2006; Salami, Eriksson, & Nyberg, 2012), or even more general accounts that assume the engagement of supplementary networks to preserve cognitive function in the face of diffuse neurofunctional decline (Park & Reuter-Lorenz, 2009; Reuter-Lorenz & Park, 2014). Structural decline of neurotransmitter systems throughout the brain may also result in functional changes, including attenuation of neuronal gain control, resulting in suboptimal cognition (Li, Lindenberger, & Sikström, 2001; Li & Rieckmann, 2014). In fact, our results provide support for hierarchy-specific shifts, whereby diffuse structural changes result in compensatory recruitment of higher-level regions. In other words, cortical atrophy across a large territory could evoke increased functional demands on higher-order default mode and frontal–parietal networks. Though not fully understood, the increase in activity, connectivity, and metabolic stress may in turn increase the susceptibility of higher-order networks to Aβ pathology (Bero et al., 2011; Buckner, 2005; Lehmann et al., 2013). Additionally, we chose to corroborate our findings by mapping levels of laminar differentiation to our neocortical surface models. This once again revealed a diffuse aging effect on cortical thickness, while Aβ deposition was greatest in limbic transmodal areas and decreased steadily toward sensory and motor cortices. We believe this unique tripartite analysis consisting of surface-based models, connectome gradient profiling, and laminar differentiation analysis serves to further highlight the vulnerability of the neocortex to atrophy and pathological deposits in healthy aging. We believe this framework could be leveraged in future research to further explore structural and functional decline in neurodegenerative diseases. Regarding the hippocampal long-axis gradient, we observed larger age-related volume loss toward the posterior end, supporting earlier literature demonstrating a vulnerability of the posterior hippocampus in aging (Kalpouzos, Chételat, Baron, et al., 2009; Nordin et al., 2018; Pruessner, Collins, Pruessner, & Evans, 2001). We found no significant effect of age on hippocampal Aβ deposition across the entire hippocampal gradient, which is in keeping with our regional findings demonstrating only trends for increased deposition in the hippocampal head. We believe our lack of significant findings relating to Aβ across the hippocampus could be the result of low sensitivity of PET imaging to Aβ deposition in this structure. The unique anatomy of the hippocampal formation, coupled with its predisposition toward partial volume errors, has been hypothesized to reduce the reliability of PET imaging in this region (Sabri, Seibyl, Rowe, & Barthel, 2015). Nevertheless, we deemed it worthwhile to explore hippocampal Aβ, given theoretical benefits when studying metabolic data with subfield-surface analytics that offer reduced partial volume effect during parameter sampling and high spatial specificity.

With regards to the cognitive substrates of our findings, thickness reductions across the neocortical gradient related to lower scores on measures of episodic memory and fluid intelligence, supporting a contribution of whole-cortex morphological integrity to this faculty (Fjell et al., 2006; Schretlen et al., 2000). As effect sizes were somewhat higher in unimodal portions of the gradient, our data may underline the contribution of externally-oriented attention networks to fluid intelligence (Majerus et al., 2012), with particularly the dorsal attention network being proximal to sensory and sensorimotor anchors on the neocortical gradient (Margulies et al., 2016). The dorsal attentional network and sensorimotor regions are densely interconnected, and previous research has shown that externally-oriented operations broadly contribute to fluid intelligence (Hearne, Mattingley, & Cocchi, 2016). Our findings demonstrating reduced thickness and volume along the neocortical and hippocampal gradient to be associated to cognitive decline supports previous literature indicating such relations across different cognitive domains (Fjell et al., 2006; Leal & Yassa, 2015; Mielke et al., 2012; Walhovd et al., 2006). Furthermore, earlier work has somewhat struggled to establish associations between specific cognitive functions and morphometric characteristics of brain regions known to be functionally involved, such as the hippocampus/parahippocampal region in episodic memory (Reitz et al., 2009; van Petten, 2004; Ziegler et al., 2010). However, several studies have shown significant relationships between the morphology of mesiotemporal structures and related cognitive processes in aging (Kalpouzos, Chételat, Landeau, et al., 2009; Walhovd et al., 2004; Yonelinas et al., 2007). In support of this, we observed reduced hippocampal volume in both our surface- and gradient-based analysis to correlate with reduced scores on tests pertaining to episodic memory. The presence of such brain structure-cognition relationships may strengthen the argument that reductions in cognitive performance observed in healthy aging can, in part, be explainable by structural decline of associated brain regions. However, it should be noted that future studies employing longitudinal designs, larger samples, and multiple scanning points are required to ultimately establish cause and effect.

With respect to Aβ, particularly transmodal neocortical increases related to worse scores, with effects significant for fluid intelligence but only trending for memory-related factor scores. Previous work has highlighted a relationship between Aβ deposition and poorer performance on several aspects of cognition including processing speed and fluid reasoning (Rodrigue et al., 2012). Our results build upon these findings by demonstrating increased Aβ deposition in transmodal portions of the gradient to be associated with lower fluid intelligence scores, in accordance with the proposed involvement of the prefrontal and parietal cortex in this cognitive domain (Gray, Chabris, & Braver, 2003). This result has important implications for aging research as it suggests that cognitive dysfunction could also occur in the preclinical phase of Alzheimer's Disease, which is characterized by the presence of Aβ but without the associated cognitive decline (Sperling et al., 2011). In contrast, we found no significant effect on measures of episodic memory, in keeping with previous

literature (Aizenstein et al., 2008; Jack et al., 2008; Rodrigue et al., 2012; Sperling et al., 2009); hypothetically, longitudinal decline in memory may be more sensitive to Aβ than cross-sectional estimates (Resnick et al., 2010; Storandt, Mintun, Head, & Morris, 2009). Although the evidence for a relationship existing between Aβ deposition and cognitive decline in healthy individuals continues to be mixed, the importance of Aβ imaging in cognitively healthy individuals remains due to its potential as a biomarker for clinical progression (Huijbers et al., 2015; Klunk, 2011). Although not explored here, the observed structural and metabolic change across neocortical and hippocampal regions may reflect disruptions of large-scale networks, negatively affecting cognitive functions. In support of this, we incorporated a multivariate PLS analysis, associating brain and phenotypic measures, which revealed a cohesive pattern of regions showing metabolic and structural imaging changes coupled to aging and general cognitive decline. Findings were significant after thousands of permutations, and replicable across hundreds of cross-validation experiments, supporting robustness. In further agreement to network-level effects, previous work indeed showed a decline in white matter network efficiency with age (Collin & Van Den Heuvel, 2013; Zhao et al., 2015), with long-range connections and higher-order cognitive networks demonstrating considerable vulnerability (Montembeault et al., 2012; Spreng & Turner, 2013; Tomasi & Volkow, 2012).

When controlling for APOEe4 genotype status, we observed no modulation or differences in cognitive scores unlike recent data indicative of a significant effect of genotype status on cognition in aging (Schiepers et al., 2012). One potential explanation for the lack of sensitivity is the relatively small sample of APOEe4 carriers (n = 23) in this current study. However, our results do lend support to earlier work demonstrating no effect of APOEe4 status on cognition in healthy aging (Mayeux, Small, Tang, Tycko, & Stern, 2001; Pendleton et al., 2002; Small et al., 2000; Small, Basun, & Bäckman, 1998; Smith et al., 1998). Furthermore, in studies that do find an effect of APOEe4 on cognition, the effect is not consistent across cognitive domains, with attention, working memory, verbal ability, visuospatial skill, and perceptual speed demonstrating no significant deficits as a result of genotype status (Small, Rosnick, Fratiglioni, & Bäckman, 2004; Wisdom, Callahan, & Hawkins, 2011).

A potential limitation to this study is that we were unable to control for SCD. SCD was assessed in the DLBS using the Metamemory in Adulthood questionnaire (Chen, Farrell, Moore, & Park, 2019), however, this data has yet to be released. SCD has been related to mesiotemporal atrophy, functional connectivity alterations, decreased task-directed attention, and increased white matter hyperintensities (Fan et al., 2018; Hayes et al., 2017; Van Rooden et al., 2018; Verfaillie et al., 2018; Viviano et al., 2019), and might thus have been an interesting variable to relate to neocortical and hippocampal measures in the newly proposed gradient space. Furthermore, the DLBS only screened against physical health, neurological health, and MMSE>26 to cover a large range of individuals falling under a healthy aging umbrella. Measures of preclinical Alzheimer's Disease, including Amyloid beta SUVR cut-off points and/or Scheltens visual rating scale for mesiotemporal atrophy (Scheltens et al., 1995) were thus not used for subject exclusion. It is, therefore, possible that some participants might have suffered from preclinical stages of Alzheimer's Disease with still high MMSE scores. Finally, we restricted our analysis to 102/144 cases with higher-quality MRI data. Although this nominally reduced statistical power, focusing on cases with high-quality imaging data and quality-controlled hippocampal and cortical segmentations may improve inference. In fact, it might even be more sensitive than an assessment of a larger dataset with potential confounds in image quality and surface extractions.

In conclusion, our work presents a novel approach to represent age-related differences in brain structure, metabolism, and cognition. In addition to supporting previous work indicative of structural and metabolic change in the aging brain, the use of a compact analytical framework to relate brain-based biomarkers to macroscale functional systems allowed for novel insights into the interplay between pathological deposits and structural compromise, and how this subsequently impacts upon cognition in the healthy aging population.

ACKNOWLEDGMENTS

We like to thank the investigators of the DLBS and associated funding sources for making their data available, and INDI/FCP1000 for hosting the imaging data. Dr. Casey Paquola was supported by the Transforming Autism Care Consortium. Reinder Vos de Wael, MSc was supported by the Savoy Foundation for Epilepsy Research. Sara Larivière, MSc was supported by a FRQS Fellowship. Drs. Neda and Andrea Bernasconi were funded by the Canadian Institutes of Health Research (CIHR) and received salary support from the Fonds de la Recherche du Quebec—Santé (FRQS). Dr. Boris Bernhardt acknowledges research support from the National Science and Engineering Research Council of Canada (NSERC Discovery-1304413), CIHR (FDN-154298), SickKids Foundation (NI17-039), as well as salary support from the FRQS (Junior 1 Research Scholar). Dr. R. Nathan Spreng is supported by NSERC, CIHR, as well as salary support from the FRQS.

DATA AND CODE AVAILABILITY

All data are based on the openly-shared Dallas Lifespan Brain Study dataset, available under http://fcon_1000.projects.nitrc.org/indi/retro/dlbs.html. Preprocessed and quality-controlled surface feature data are available upon request. Surface-wide statistical comparisons were carried out using SurfStat for Matlab (http://mica-mni.github.io/surfstat). Gradient mapping tools used in this work are available via https://github.com/MICA-MNI/micaopen/diffusion_map_embedding.

ORCID

Sara Lariviere https://orcid.org/0000-0001-5701-1307
R. Nathan Spreng https://orcid.org/0000-0003-1530-8916
Boris C. Bernhardt https://orcid.org/0000-0001-9256-6041

REFERENCES

Abdi, H., & Williams, L. J. (2010). Principal component analysis. *Wiley Interdisciplinary Reviews: Computational Statistics*, *2*(4), 433–459. https://doi.org/10.1002/wics.101

Aizenstein, H. J., Nebes, R. D., Saxton, J. A., Price, J. C., Mathis, C. A., Tsopelas, N. D., … Klunk, W. E. (2008). Frequent amyloid deposition without significant cognitive impairment among the elderly. *Archives of Neurology*, *65*(11), 1509–1517. https://doi.org/10.1001/archneur.65.11.1509

Andrews-Hanna, J. R., Snyder, A. Z., Vincent, J. L., Lustig, C., Head, D., Raichle, M. E., & Buckner, R. L. (2007). Disruption of large-scale brain systems in advanced aging. *Neuron*, *56*(5), 924–935. https://doi.org/10.1016/j.neuron.2007.10.038

Baciu, M., Boudiaf, N., Cousin, E., Perrone-Bertolotti, M., Pichat, C., Fournet, N., … Krainik, A. (2016). Functional MRI evidence for the decline of word retrieval and generation during normal aging. *Age*, *38*(1), 1–22. https://doi.org/10.1007/s11357-015-9857-y

Bajaj, S., Alkozei, A., Dailey, N. S., & Killgore, W. D. S. (2017). Brain aging: Uncovering cortical characteristics of healthy aging in young adults. *Frontiers in Aging Neuroscience*, *9*, 412. https://doi.org/10.3389/fnagi.2017.00412

Baker, J. E., Lim, Y. Y., Pietrzak, R. H., Hassenstab, J., Snyder, P. J., Masters, C. L., & Maruff, P. (2017). Cognitive impairment and decline in cognitively normal older adults with high amyloid-β: A meta-analysis. *Alzheimer's and Dementia*, *6*, 108–121. https://doi.org/10.1016/j.dadm.2016.09.002

Benjamini, Y., & Hochberg, Y. (1995). Controlling the false discovery rate: A practical and powerful approach to multiple testing. *Journal of the Royal Statistical Society*, *57*(1), 289–300. https://doi.org/10.2307/2346101

Bernhardt, B. C., Bernasconi, A., Liu, M., Hong, S.-J., Caldairou, B., Goubran, M., … Bernasconi, N. (2016). The spectrum of structural and functional imaging abnormalities in temporal lobe epilepsy. *Annals of Neurology*, *80*(1), 142–153. https://doi.org/10.1002/ana.24691

Bernhardt, B. C., Fadaie, F., De Wael, R. V., Hong, S. J., Liu, M., Guiot, M. C., … Bernasconi, N. (2017). Preferential susceptibility of limbic cortices to microstructural damage in temporal lobe epilepsy: A quantitative T1 mapping study. *NeuroImage*, *182*, 294–303. https://doi.org/10.1016/j.neuroimage.2017.06.002

Bero, A. W., Yan, P., Roh, J. H., Cirrito, J. R., Stewart, F. R., Raichle, M. E., … Holtzman, D. M. (2011). Neuronal activity regulates the regional vulnerability to amyloid-2 deposition. *Nature Neuroscience*, *14*(6), 750–756. https://doi.org/10.1038/nn.2801

Bilgel, M., An, Y., Helphrey, J., Elkins, W., Gomez, G., Wong, D. F., … Resnick, S. M. (2018). Effects of amyloid pathology and neurodegeneration on cognitive change in cognitively normal adults. *Brain*, *141*(8), 2475–2485. https://doi.org/10.1093/brain/awy150

Brandt, J. (1991). The Hopkins verbal learning test: Development of a new memory test with six equivalent forms. *The Clinical Neuropsychologist*, *5*(2), 125–142. https://doi.org/10.1080/13854049108403297

Buckner, R. L. (2004). Memory and executive function in aging and ad: Multiple factors that cause decline and reserve factors that compensate. *Neuron*, *44*(1), 195–208. https://doi.org/10.1016/j.neuron.2004.09.006

Buckner, R. L. (2005). Molecular, structural, and functional characterization of Alzheimer's disease: Evidence for a relationship between default activity, amyloid, and memory. *Journal of Neuroscience*, *25*(34), 7709–7717. https://doi.org/10.1523/JNEUROSCI.2177-05.2005

Buckner, R. L., Andrews-Hanna, J. R., & Schacter, D. L. (2008). The brain's default network: Anatomy, function, and relevance to disease. *Annals of the New York Academy of Sciences*, *1124*, 1–38. https://doi.org/10.1196/annals.1440.011

Buckner, R. L., & Krienen, F. M. (2013). The evolution of distributed association networks in the human brain. *Trends in Cognitive Sciences*, *17*(12), 648–665. https://doi.org/10.1016/j.tics.2013.09.017

Buckner, R. L., Sepulcre, J., Talukdar, T., Krienen, F. M., Liu, H., Hedden, T., … Johnson, K. A. (2009). Cortical hubs revealed by intrinsic functional connectivity: Mapping, assessment of stability, and relation to Alzheimer's Disease. *Journal of Neuroscience*, *29*(6), 1860–1873. https://doi.org/10.1523/JNEUROSCI.5062-08.2009

Caldairou, B., Bernhardt, B. C., Kulaga-Yoskovitz, J., Kim, H., Bernasconi, N., & Bernasconi, A. (2016). A surface patch-based segmentation method for hippocampal subfields. *Lecture notes in computer science (including subseries lecture notes in artificial intelligence and lecture notes in bioinformatics)* (Vol. 9901, pp. 379–387). LNCS. https://doi.org/10.1007/978-3-319-46723-8_44

Cardinale, F., Chinnici, G., Bramerio, M., Mai, R., Sartori, I., Cossu, M., … Ferrigno, G. (2014). Validation of FreeSurfer-estimated brain cortical thickness: Comparison with histologic measurements. *Neuroinformatics*, *12*(4), 535–542. https://doi.org/10.1007/s12021-014-9229-2

Chen, X., Farrell, M. E., Moore, W., & Park, D. C. (2019). Actual memory as a mediator of the amyloid-subjective cognitive decline relationship. *Alzheimer's and Dementia: Diagnosis, Assessment and Disease Monitoring*, *11*, 151–160. https://doi.org/10.1016/j.dadm.2018.12.007

Cohen, A. L., Fair, D. A., Dosenbach, N. U. F., Miezin, F. M., Dierker, D., Van Essen, D. C., … Petersen, S. E. (2008). Defining functional areas in individual human brains using resting functional connectivity MRI. *NeuroImage*, *41*(1), 45–57. https://doi.org/10.1016/j.neuroimage.2008.01.066

Collin, G., & Van Den Heuvel, M. P. (2013). The ontogeny of the human connectome: Development and dynamic changes of brain connectivity across the life span. *The Neuroscientist*, *19*(6), 616–628. https://doi.org/10.1177/1073858413503712

Dale, A. M., Fischl, B., & Sereno, M. I. (1999). Cortical surface-based analysis: I. segmentation and surface reconstruction. *NeuroImage*, *9*(2), 179–194. https://doi.org/10.1006/nimg.1998.0395

Davis, S. W., Dennis, N. A., Daselaar, S. M., Fleck, M. S., & Cabeza, R. (2008). Qué PASA? The posterior-anterior shift in aging. *Cerebral Cortex*, *18*(5), 1201–1209. https://doi.org/10.1093/cercor/bhm155

de Flores, R., La Joie, R., & Chételat, G. (2015). Structural imaging of hippocampal subfields in healthy aging and Alzheimer's disease. *Neuroscience*, *309*, 29–50. https://doi.org/10.1016/j.neuroscience.2015.08.033

Draganski, B., Lutti, A., & Kherif, F. (2013). Impact of brain aging and neurodegeneration on cognition: Evidence from MRI. *Current Opinion in Neurology*, *26*(6), 640–645. https://doi.org/10.1097/WCO.0000000000000029

Eickhoff, S. B., Yeo, B. T. T., & Genon, S. (2018). Imaging-based parcellations of the human brain. *Nature Reviews Neuroscience*, *19*, 627–686. https://doi.org/10.1038/s41583-018-0071-7

Ekstrom, R. B. R., French, J. J. W., Harman, H. H., & Dermen, D. (1976). From the cover: Training, maturation, and genetic influences on the development of executive attention. In *Manual for kit of factor-referenced cognitive tests*. Princeton, NJ: Educational Testing Service. https://doi.org/10.1073/pnas.0506897102

Elman, J. A., Madison, C. M., Baker, S. L., Vogel, J. W., Marks, S. M., Crowley, S., … Jagust, W. J. (2016). Effects of Beta-amyloid on resting state functional connectivity within and between networks reflect known patterns of regional vulnerability. *Cerebral Cortex*, *26*(2), 695–707. https://doi.org/10.1093/cercor/bhu259

Fan, L. Y., Lai, Y. M., Chen, T. F., Hsu, Y. C., Chen, P. Y., Huang, K. Z., … Chiu, M. J. (2018). Diminution of context association memory structure in subjects with subjective cognitive decline. *Human Brain Mapping*, *39*(6), 2549–2562. https://doi.org/10.1002/hbm.24022

Farrell, M. E., Kennedy, K. M., Rodrigue, K. M., Wig, G., Bischof, G. N., Rieck, J. R., … Park, D. C. (2017). Association of longitudinal cognitive decline with amyloid burden in middle-aged and older adults: Evidence

for a dose-response relationship. *JAMA Neurology*, *74*(7), 830–838. https://doi.org/10.1001/jamaneurol.2017.0892

Ferreira, L. K., Regina, A. C. B., Kovacevic, N., Martin, M. D. G. M., Santos, P. P., Carneiro, C. D. G., … Busatto, G. F. (2016). Aging effects on whole-brain functional connectivity in adults free of cognitive and psychiatric disorders. *Cerebral Cortex*, *26*(9), 3851–3865. https://doi.org/10.1093/cercor/bhv190

Fischl, B., & Dale, A. M. (2000). Measuring the thickness of the human cerebral cortex from magnetic resonance images. *Proceedings of the National Academy of Sciences*, *97*(20), 11050–11055. https://doi.org/10.1073/pnas.200033797

Fischl, B., Sereno, M. I., & Dale, A. M. (1999). Cortical surface-based analysis: II. Inflation, flattening, and a surface-based coordinate system. *NeuroImage*, *9*, 195–207. https://doi.org/10.1006/nimg.1998.0396

Fjell, A. M., McEvoy, L., Holland, D., Dale, A. M., & Walhovd, K. B. (2014). What is normal in normal aging? Effects of aging, amyloid and Alzheimer's disease on the cerebral cortex and the hippocampus. *Progress in Neurobiology*, *117*, 20–40. https://doi.org/10.1016/j.pneurobio.2014.02.004

Fjell, A. M., Sneve, M. H., Grydeland, H., Storsve, A. B., & Walhovd, K. B. (2017). The disconnected brain and executive function decline in aging. *Cerebral Cortex (New York, NY)*, *27*(3), 2303–2317. https://doi.org/10.1093/cercor/bhw082

Fjell, A. M., Walhovd, K. B., Fennema-Notestine, C., McEvoy, L. K., Hagler, D. J., Holland, D., … Dale, A. M. (2009). One-year brain atrophy evident in healthy aging. *Journal of Neuroscience*, *29*(48), 15223–15231. https://doi.org/10.1523/JNEUROSCI.3252-09.2009

Fjell, A. M., Walhovd, K. B., Reinvang, I., Lundervold, A., Salat, D., Quinn, B. T., … Dale, A. M. (2006). Selective increase of cortical thickness in high-performing elderly—Structural indices of optimal cognitive aging. *NeuroImage*, *29*(3), 984–994. https://doi.org/10.1016/j.neuroimage.2005.08.007

Folstein, M. F., Folstein, S. E., & McHugh, P. R. (1975). "Mini-mental state". A practical method for grading the cognitive state of patients for the clinician. *Journal of Psychiatric Research*, *12*(3), 189–198. https://doi.org/10.1016/0022-3956

Fox, M. D., Snyder, A. Z., Vincent, J. L., Corbetta, M., Van Essen, D. C., & Raichle, M. E. (2005). From the cover: The human brain is intrinsically organized into dynamic, anticorrelated functional networks. *Proceedings of the National Academy of Sciences*, *102*(27), 9673–9678. https://doi.org/10.1073/pnas.0504136102

Fraser, M. A., Shaw, M. E., & Cherbuin, N. (2015). A systematic review and meta-analysis of longitudinal hippocampal atrophy in healthy human ageing. *NeuroImage*, *112*, 364–374. https://doi.org/10.1016/j.neuroimage.2015.03.035

Grady, C. L., Maisog, J. M., Horwitz, B., Ungerleider, L. G., Mentis, M. J., Salerno, J. A., … Haxby, J. V. (1994). Age-related changes in cortical blood flow activation during visual processing of faces and location. *The Journal of Neuroscience*, *13*, 257–278. https://doi.org/10.1080/09541440042000304

Gray, J. R., Chabris, C. F., & Braver, T. S. (2003). Neural mechanisms of general fluid intelligence. *Nature Neuroscience*, *6*(3), 316–322. https://doi.org/10.1038/nn1014

Greve, D. N., & Fischl, B. (2009). Accurate and robust brain image alignment using boundary-based registration. *NeuroImage*, *48*(1), 63–72. https://doi.org/10.1016/j.neuroimage.2009.06.060

Harman, H. H. (1976). *Modern factor analysis*. Chicago, IL: Chicago University Press.

Hatanpaa, K. J., Raisanen, J. M., Herndon, E., Burns, D. K., Foong, C., Habib, A. A., & White, C. L. (2014). Hippocampal sclerosis in dementia, epilepsy, and ischemic injury: Differential vulnerability of hippocampal subfields. *Journal of Neuropathology and Experimental Neurology*, *73*(2), 136–142. https://doi.org/10.1097/OPX.0000000000000170

Hayes, J. M., Tang, L., Viviano, R. P., van Rooden, S., Ofen, N., & Damoiseaux, J. S. (2017). Subjective memory complaints are associated with brain activation supporting successful memory encoding. *Neurobiology of Aging*, *60*, 71–80. https://doi.org/10.1016/j.neurobiolaging.2017.08.015

He, X., Qin, W., Liu, Y., Zhang, X., Duan, Y., Song, J., … Yu, C. (2014). Abnormal salience network in normal aging and in amnestic mild cognitive impairment and Alzheimer's disease. *Human Brain Mapping*, *35*(7), 3446–3464. https://doi.org/10.1002/hbm.22414

Hearne, L. J., Mattingley, J. B., & Cocchi, L. (2016). Functional Brain Networks Related to Individual Differences in Human Intelligence at Rest. *Scientific Reports*, *6*, 6. https://doi.org/10.1038/srep32328

Heywood, H. B. (1931). On Finite Sequences of Real Numbers. *Proceedings of the Royal Society A: Mathematical, Physical and Engineering Sciences*, *134*(824), 486–501. https://doi.org/10.1098/rspa.1931.0209

Hong, S. J., de Wael, R. V., Bethlehem, R. A. I., Lariviere, S., Paquola, C., Valk, S. L., … Bernhardt, B. C. (2019). A typical functional connectome hierarchy in autism. *Nature Communications*, *10*(1), 1022–1035. https://doi.org/10.1038/s41467-019-08944-1

Huijbers, W., Mormino, E. C., Schultz, A. P., Wigman, S., Ward, A. M., Larvie, M., … Sperling, R. A. (2015). Amyloid-β deposition in mild cognitive impairment is associated with increased hippocampal activity, atrophy and clinical progression. *Brain*, *138*(4), 1023–1035. https://doi.org/10.1093/brain/awv007

Huntenburg, J. M., Bazin, P. L., & Margulies, D. S. (2018). Large-scale gradients in human cortical organization. *Trends in Cognitive Sciences*, *22*(1), 21–31. https://doi.org/10.1016/j.tics.2017.11.002

Jack, C. R., Lowe, V. J., Senjem, M. L., Weigand, S. D., Kemp, B. J., Shiung, M. M., … Petersen, R. C. (2008). 11C PiB and structural MRI provide complementary information in imaging of Alzheimer's disease and amnestic mild cognitive impairment. *Brain*, *131*(3), 665–680. https://doi.org/10.1093/brain/awm336

Jansen, W. J., Ossenkoppele, R., Knol, D. L., Tijms, B. M., Scheltens, P., Verhey, F. R. J., … Zetterberg, H. (2015). Prevalence of cerebral amyloid pathology in persons without dementia: A meta-analysis. *JAMA*, *313*(19), 1924–1938. https://doi.org/10.1001/jama.2015.4668

Jansen, W. J., Ossenkoppele, R., Tijms, B. M., Fagan, A. M., Hansson, O., Klunk, W. E., … Zetterberg, H. (2018). Association of cerebral amyloid-β aggregation with cognitive functioning in persons without dementia. *JAMA Psychiatry*, *75*(1), 84–95. https://doi.org/10.1001/jamapsychiatry.2017.3391

Kalpouzos, G., Chételat, G., Baron, J. C., Landeau, B., Mevel, K., Godeau, C., … Desgranges, B. (2009). Voxel-based mapping of brain gray matter volume and glucose metabolism profiles in normal aging. *Neurobiology of Aging*, *30*(1), 112–124. https://doi.org/10.1016/j.neurobiolaging.2007.05.019

Kalpouzos, G., Chételat, G., Landeau, B., Clochon, P., Viader, F., Eustache, F., & Desgranges, B. (2009). Structural and metabolic correlates of episodic memory in relation to the depth of encoding in normal aging. *Journal of Cognitive Neuroscience*, *21*(2), 372–389. https://doi.org/10.1162/jocn.2008.21027

Kiebel, S. J., Daunizeau, J., & Friston, K. J. (2008). A hierarchy of timescales and the brain. *PLoS Computational Biology*, *4*(11), e1000209. https://doi.org/10.1371/journal.pcbi.1000209

Kim, H., Bernhardt, B. C., Kulaga-Yoskovitz, J., Caldairou, B., Bernasconi, A., & Bernasconi, N. (2014). Multivariate hippocampal subfield analysis of local MRI intensity and volume: Application to temporal lobe epilepsy. *Lecture notes in computer science (including subseries lecture notes in artificial intelligence and lecture notes in bioinformatics)*, (Vol. 8674, pp. 170–178). LNCS (PART 2). https://doi.org/10.1007/978-3-319-10470-6_22

Klunk, W. E. (2011). Amyloid imaging as a biomarker for cerebral β-amyloidosis and risk prediction for Alzheimer dementia. *Neurobiology of Aging*, *32*(Suppl 1), 20–36. https://doi.org/10.1016/j.neurobiolaging.2011.09.006

Knopman, D. S., Lundt, E. S., Therneau, T. M., Vemuri, P., Lowe, V. J., Kantarci, K., … Jack, C. R. (2018). Joint associations of β-amyloidosis

and cortical thickness with cognition. *Neurobiology of Aging*, *65*, 121–131. https://doi.org/10.1016/j.neurobiolaging.2018.01.017

Kulaga-Yoskovitz, J., Bernhardt, B. C., Hong, S. J., Mansi, T., Liang, K. E., Van Der Kouwe, A. J. W., … Bernasconi, N. (2015). Multi-contrast submillimetric 3 Tesla hippocampal subfield segmentation protocol and dataset. *Scientific Data*, *2*, 150059. https://doi.org/10.1038/sdata.2015.59

Kuperberg, G. R., Broome, M. R., McGuire, P. K., David, A. S., Eddy, M., Ozawa, F., … Fischl, B. (2003). Regionally localized thinning of the cerebral cortex in schizophrenia. *Archives of General Psychiatry*, *60*(9), 878–888. https://doi.org/10.1001/archpsyc.60.9.878

Leal, S. L., & Yassa, M. A. (2015). Neurocognitive aging and the Hippocampus across species. *Trends in Neurosciences*, *38*(12), 800–812. https://doi.org/10.1016/j.tins.2015.10.003

Lehmann, M., Madison, C. M., Ghosh, P. M., Seeley, W. W., Mormino, E., Greicius, M. D., … Rabinovici, G. D. (2013). Intrinsic connectivity networks in healthy subjects explain clinical variability in Alzheimer's disease. *Proceedings of the National Academy of Sciences*, *110*(28), 11606–11611. https://doi.org/10.1073/pnas.1221536110

Li, S. C., Lindenberger, U., & Sikström, S. (2001). Aging cognition: From neuromodulation to representation. *Trends in Cognitive Sciences*, *5*(11), 479–486. https://doi.org/10.1016/S1364-6613

Li, S. C., & Rieckmann, A. (2014). Neuromodulation and aging: Implications of aging neuronal gain control on cognition. *Current Opinion in Neurobiology*, *29*, 148–158. https://doi.org/10.1016/j.conb.2014.07.009

Lim, H. K., Nebes, R., Snitz, B., Cohen, A., Mathis, C., Price, J., … Aizenstein, H. J. (2014). Regional amyloid burden and intrinsic connectivity networks in cognitively normal elderly subjects. *Brain*, *137*(12), 3327–3338. https://doi.org/10.1093/brain/awu271

López-Otín, C., Blasco, M. A., Partridge, L., Serrano, M., & Kroemer, G. (2013). The hallmarks of aging. *Cell*, *153*(6), 1194–1217. https://doi.org/10.1016/j.cell.2013.05.039

Majerus, S., Attout, L., D'Argembeau, A., Degueldre, C., Fias, W., Maquet, P., … Balteau, E. (2012). Attention supports verbal short-term memory via competition between dorsal and ventral attention networks. *Cerebral Cortex*, *22*(5), 1086–1097. https://doi.org/10.1093/cercor/bhr174

Malykhin, N. V., Huang, Y., Hrybouski, S., & Olsen, F. (2017). Differential vulnerability of hippocampal subfields and anteroposterior hippocampal subregions in healthy cognitive aging. *Neurobiology of Aging*, *59*, 121–134. https://doi.org/10.1016/j.neurobiolaging.2017.08.001

Margulies, D. S., Ghosh, S. S., Goulas, A., Falkiewicz, M., Huntenburg, J. M., Langs, G., … Smallwood, J. (2016). Situating the default-mode network along a principal gradient of macroscale cortical organization. *Proceedings of the National Academy of Sciences*, *113*(44), 12574–12579. https://doi.org/10.1073/pnas.1608282113

Mayeux, R., Small, S. A., Tang, M. X., Tycko, B., & Stern, Y. (2001). Memory performance in healthy elderly without Alzheimer's disease: Effects of time and apolipoprotein-E. *Neurobiology of Aging*, *22*(4), 683–689. https://doi.org/10.1016/S0197-4580

McConathy, J., & Sheline, Y. I. (2015). Imaging biomarkers associated with cognitive decline: A review. *Biological Psychiatry*, *77*(8), 685–692. https://doi.org/10.1016/j.biopsych.2014.08.024

McGinnis, S. M., Brickhouse, M., Pascual, B., & Dickerson, B. C. (2011). Age-related changes in the thickness of cortical zones in humans. *Brain Topography*, *24*(3–4), 279–291. https://doi.org/10.1007/s10548-011-0198-6

McIntosh, A. R., & Lobaugh, N. J. (2004). Partial least squares analysis of neuroimaging data: Applications and advances. *NeuroImage*, *23*(Suppl 1), 250–263. https://doi.org/10.1016/j.neuroimage.2004.07.020

McIntosh, A. R., & Mišić, B. (2013). Multivariate statistical analyses for neuroimaging data. *Annual Review of Psychology*, *64*, 499–525. https://doi.org/10.1146/annurev-psych-113011-143804

Mesulam, M. M. (1998). From sensation to cognition. *Brain*, *121*(6), 1013–1052. https://doi.org/10.1093/brain/121.6.1013

Mielke, M. M., Okonkwo, O. C., Oishi, K., Mori, S., Tighe, S., Miller, M. I., … Lyketsos, C. G. (2012). Fornix integrity and hippocampal volume predict memory decline and progression to Alzheimer's disease. *Alzheimer's and Dementia*, *8*(2), 105–113. https://doi.org/10.1016/j.jalz.2011.05.2416

Montembeault, M., Joubert, S., Doyon, J., Carrier, J., Gagnon, J. F., Monchi, O., … Brambati, S. M. (2012). The impact of aging on gray matter structural covariance networks. *NeuroImage*, *63*(2), 754–759. https://doi.org/10.1016/j.neuroimage.2012.06.052

Mortamais, M., Ash, J. A., Harrison, J., Kaye, J., Kramer, J., Randolph, C., … Ritchie, K. (2017). Detecting cognitive changes in preclinical Alzheimer's disease: A review of its feasibility. *Alzheimer's and Dementia*, *13*(4), 468–492. https://doi.org/10.1016/j.jalz.2016.06.2365

Murphy, C., Jefferies, E., Rueschemeyer, S. A., Sormaz, M., Wang, H. T., Margulies, D. S., & Smallwood, J. (2018). Distant from input: Evidence of regions within the default mode network supporting perceptually-decoupled and conceptually-guided cognition. *NeuroImage*, *171*, 393–401. https://doi.org/10.1016/j.neuroimage.2018.01.017

Mutlu, J., Landeau, B., Gaubert, M., De La Sayette, V., Desgranges, B., & Chételat, G. (2017). Distinct influence of specific versus global connectivity on the different Alzheimer's disease biomarkers. *Brain*, *140*(12), 3317–3328. https://doi.org/10.1093/brain/awx279

Myers, N., Pasquini, L., Göttler, J., Grimmer, T., Koch, K., Ortner, M., … Sorg, C. (2014). Within-patient correspondence of amyloid-β and intrinsic network connectivity in Alzheimer's disease. *Brain*, *137*(7), 2052–2064. https://doi.org/10.1093/brain/awu103

Nordin, K., Persson, J., Stening, E., Herlitz, A., Larsson, E. M., & Söderlund, H. (2018). Structural whole-brain covariance of the anterior and posterior hippocampus: Associations with age and memory. *Hippocampus*, *28*(2), 151–163. https://doi.org/10.1002/hipo.22817

Palmqvist, S., Schöll, M., Strandberg, O., Mattsson, N., Stomrud, E., Zetterberg, H., … Hansson, O. (2017). Earliest accumulation of β-amyloid occurs within the default-mode network and concurrently affects brain connectivity. *Nature Communications*, *8*(1), 1214. https://doi.org/10.1038/s41467-017-01150-x

Pan, C.-W., Wang, X., Ma, Q., Sun, H.-P., Xu, Y., & Wang, P. (2015). Cognitive dysfunction and health-related quality of life among older Chinese. *Scientific Reports*, *5*(1), 17301. https://doi.org/10.1038/srep17301

Paquola, C., Vos De Wael, R., Wagstyl, K., Bethlehem, R. A. I., Hong, S.-J., Seidlitz, J., … Bernhardt, B. C. (2019). Microstructural and functional gradients are increasingly dissociated in transmodal cortices. *PLoS Biology*, *17*(5), e3000284. https://doi.org/10.1371/journal.pbio.3000284

Park, D. C. (2018). *Dallas lifespan brain study*. Retrieved from http://fcon_1000.projects.nitrc.org/indi/retro/dlbs.html.

Park, D. C., & Reuter-Lorenz, P. (2009). The adaptive brain: Aging and neurocognitive scaffolding. *Annual Review of Psychology*, *60*(1), 173–196. https://doi.org/10.1146/annurev.psych.59.103006.093656

Payer, D., Marshuetz, C., Sutton, B., Hebrank, A., Welsh, R. C., & Park, D. C. (2006). Decreased neural specialization in old adults on a working memory task. *Neuroreport*, *17*(5), 487–491. https://doi.org/10.1097/01.wnr.0000209005.40481.31

Pendleton, N., Payton, A., van den Boogerd, E. H., Holland, F., Diggle, P., Rabbitt, P. M. A., … Ollier, W. E. R. (2002). Apolipoprotein E genotype does not predict decline in intelligence in healthy older adults. *Neuroscience Letters*, *324*(1), 74–76. https://doi.org/10.1016/S0304-3940(02)00135-0

Plachti, A., Eickhoff, S. B., Hoffstaedter, F., Patil, K. R., Laird, A. R., Fox, P. T., … Genon, S. (2019). Multimodal Parcellations and Extensive Behavioral Profiling Tackling the Hippocampus Gradient. *Cerebral Cortex*, *bhy336*. https://doi.org/10.1093/cercor/bhy336

Poppenk, J., Evensmoen, H. R., Moscovitch, M., & Nadel, L. (2013). Long-axis specialization of the human hippocampus. *Trends in Cognitive Sciences*, *17*(5), 230–240. https://doi.org/10.1016/j.tics.2013.03.005

Pruessner, J. C., Collins, D. L., Pruessner, M., & Evans, A. C. (2001). Age and gender predict volume decline in the anterior and posterior hippocampus in early adulthood. *The Journal of Neuroscience*, *21*(1), 194–200. https://doi.org/10.1523/JNEUROSCI.21-01-00194.2001

Rapoport, S. I. (1989). Hypothesis: Alzheimer's disease is a phylogenetic disease. *Medical Hypotheses*, *29*(3), 147–150. https://doi.org/10.1016/0306-9877(89)90185-0

Raven, J. C. (1996). *Standard progressive matrices: Sets A, B, C, D & E*. Oxfod, UK: Oxford Psychologists Press.

Reitz, C., Brickman, A. M., Brown, T. R., Manly, J., DeCarli, C., Small, S. A., & Mayeux, R. (2009). Linking hippocampal structure and function to memory performance in an aging population. *Archives of Neurology*, *66*(11), 1385–1392. https://doi.org/10.1001/archneurol.2009.214

Resnick, S. M., Sojkova, J., Zhou, Y., An, Y., Ye, W., Holt, D. P., … Wong, D. F. (2010). Longitudinal cognitive decline is associated with fibrillar amyloid-beta measured by [11C]PiB. *Neurology*, *74*(10), 807–815. https://doi.org/10.1212/WNL.0b013e3181d3e3e9

Reuter-Lorenz, P. A., & Park, D. C. (2014). How does it STAC up? Revisiting the scaffolding theory of aging and cognition. *Neuropsychology Review*, *24*(3), 355–370. https://doi.org/10.1007/s11065-014-9270-9

Robbins, T. W., James, M., Owen, A. M., Sahakian, B. J., McInnes, L., & Rabbitt, P. (2010). Cambridge neuropsychological test automated battery (CANTAB): A factor analytic study of a large sample of normal elderly volunteers. *Dementia and Geriatric Cognitive Disorders*, *5*(5), 266–281. https://doi.org/10.1159/000106735

Rodrigue, K. M., Kennedy, K. M., Devous, M. D., Rieck, J. R., Hebrank, A. C., Diaz-Arrastia, R., … Park, D. C. (2012). β-amyloid burden in healthy aging: Regional distribution and cognitive consequences. *Neurology*, *78*(6), 387–395. https://doi.org/10.1212/WNL.0b013e318245d295

Rosas, H. D., Liu, A. K., Hersch, S., Glessner, M., Ferrante, R. J., Salat, D. H., … Fischl, B. (2002). Regional and progressive thinning of the cortical ribbon in Huntington's disease. *Neurology*, *58*(5), 695–701. https://doi.org/10.1212/WNL.58.5.695

Sabri, O., Seibyl, J., Rowe, C., & Barthel, H. (2015). Beta-amyloid imaging with florbetaben. *Clinical and Translational Imaging*, *3*(1), 13–26. https://doi.org/10.1007/s40336-015-0102-6

Sala-Llonch, R., Junqué, C., Arenaza-Urquijo, E. M., Vidal-Piñeiro, D., Valls-Pedret, C., Palacios, E. M., … Bartrés-Faz, D. (2014). Changes in whole-brain functional networks and memory performance in aging. *Neurobiology of Aging*, *35*(10), 2193–2202. https://doi.org/10.1016/j.neurobiolaging.2014.04.007

Salami, A., Eriksson, J., & Nyberg, L. (2012). Opposing effects of aging on large-scale brain systems for memory encoding and cognitive control. *Journal of Neuroscience*, *32*(31), 10749–10757. https://doi.org/10.1523/jneurosci.0278-12.2012

Salat, D. H., Buckner, R. L., Snyder, A. Z., Greve, D. N., Desikan, R. S. R., Busa, E., … Fischl, B. (2004). Thinning of the cerebral cortex in aging. *Cerebral Cortex*, *14*(7), 721–730. https://doi.org/10.1093/cercor/bhh032

Salthouse, T. A., & Babcock, R. L. (1991). Decomposing adult age differences in working memory. *Developmental Psychology*, *27*(5), 763–776. https://doi.org/10.1037/0012-1649.27.5.763

Sambataro, F., Murty, V. P., Callicott, J. H., Tan, H. Y., Das, S., Weinberger, D. R., & Mattay, V. S. (2010). Age-related alterations in default mode network: Impact on working memory performance. *Neurobiology of Aging*, *31*(5), 839–852. https://doi.org/10.1016/j.neurobiolaging.2008.05.022

Scheltens, P., Launer, L. J., Barkhof, F., Weinstein, H. C., & van Gool, W. A. (1995). Visual assessment of medial temporal lobe atrophy on magnetic resonance imaging: Interobserver reliability. *Journal of Neurology*, *242*(9), 557–560. https://doi.org/10.1007/BF00868807

Schiepers, O. J. G., Harris, S. E., Gow, A. J., Pattie, A., Brett, C. E., Starr, J. M., & Deary, I. J. (2012). APOE E4 status predicts age-related cognitive decline in the ninth decade: Longitudinal follow-up of the Lothian birth cohort 1921. *Molecular Psychiatry*, *17*(3), 315–324. https://doi.org/10.1038/mp.2010.137

Schretlen, D., Pearlson, G. D., Anthony, J. C., Aylward, E. H., Augustine, A. M., Davis, A., & Barta, P. (2000). Elucidating the contributions of processing speed, executive ability, and frontal lobe volume to normal age-related differences in fluid intelligence. *Journal of the International Neuropsychological Society*, *6*(1), 52–61. https://doi.org/10.1017/S1355617700611062

Shaw, M. E., Sachdev, P. S., Anstey, K. J., & Cherbuin, N. (2016). Age-related cortical thinning in cognitively healthy individuals in their 60s: The PATH through life study. *Neurobiology of Aging*, *39*, 202–209. https://doi.org/10.1016/j.neurobiolaging.2015.12.009

Small, B. J., Basun, H., & Bäckman, L. (1998). Three-year changes in cognitive performance as a function of apolipoprotein E genotype: Evidence from very old adults without dementia. *Psychology and Aging*, *13*(1), 80–87. https://doi.org/10.1037/0882-7974.13.1.80

Small, B. J., Graves, A. B., McEvoy, C. L., Crawford, F. C., Mullan, M., & Mortimer, J. A. (2000). Is APOE-ε4 a risk factor for cognitive impairment in normal aging? *Neurology*, *54*(11), 2082–2088. https://doi.org/10.1212/WNL.54.11.2082

Small, B. J., Rosnick, C. B., Fratiglioni, L., & Bäckman, L. (2004). Apolipoprotein E and cognitive performance: A meta-analysis. *Psychology and Aging*, *19*(4), 592–600. https://doi.org/10.1037/0882-7974.19.4.592

Smith, G. E., Bohac, D. L., Waring, S. C., Kokmen, E., Tangalos, E. G., Ivnik, R. J., & Petersen, R. C. (1998). Apolipoprotein E genotype influences cognitive phenotype' in patients with Alzheimer's disease but not in healthy control subjects. *Neurology*, *50*(2), 355–362. https://doi.org/10.1212/WNL.50.2.355

Sowell, E. R., Peterson, B. S., Thompson, P. M., Welcome, S. E., Henkenius, A. L., & Toga, A. W. (2003). Mapping cortical change across the human life span. *Nature Neuroscience*, *6*(3), 309–315. https://doi.org/10.1038/nn1008

Sperling, R. A., Aisen, P. S., Beckett, L. A., Bennett, D. A., Craft, S., Fagan, A. M., … Phelps, C. H. (2011). Toward defining the preclinical stages of Alzheimer's disease: Recommendations from the National Institute on Aging-Alzheimer's Association workgroups on diagnostic guidelines for Alzheimer's disease. *Alzheimer's and Dementia*, *7*(3), 280–292. https://doi.org/10.1016/j.jalz.2011.03.003

Sperling, R. A., LaViolette, P. S., O'Keefe, K., O'Brien, J., Rentz, D. M., Pihlajamaki, M., … Johnson, K. A. (2009). Amyloid deposition is associated with impaired default network function in older persons without dementia. *Neuron*, *63*(2), 178–188. https://doi.org/10.1016/j.neuron.2009.07.003

Spreng, R. N., Stevens, W. D., Chamberlain, J. P., Gilmore, A. W., & Schacter, D. L. (2010). Default network activity, coupled with the frontoparietal control network, supports goal-directed cognition. *NeuroImage*, *53*(1), 303–317. https://doi.org/10.1016/j.neuroimage.2010.06.016

Spreng, R. N., & Turner, G. R. (2013). Structural covariance of the default network in healthy and pathological aging. *Journal of Neuroscience*, *33*(38), 15226–15234. https://doi.org/10.1523/JNEUROSCI.2261-13.2013

Spreng, R. N., Wojtowicz, M. & Grady, C. (2010). Reliable differences in brain activity between young and old adults: A quantitative meta-analysis across multiple cognitive domains. *Neuroscience & Biobehavioral Reviews*, *34*(38), 1178–1194.

Steffener, J., Brickman, A. M., Habeck, C. G., Salthouse, T. A., & Stern, Y. (2013). Cerebral blood flow and gray matter volume covariance patterns of cognition in aging. *Human Brain Mapping*, *34*(12), 3267–3279. https://doi.org/10.1002/hbm.22142

Storandt, M., Mintun, M. A., Head, D., & Morris, J. C. (2009). Cognitive decline and brain volume loss as signatures of cerebral amyloid-β peptide deposition identified with Pittsburgh compound B: Cognitive

decline associated with Aβ deposition. *Archives of Neurology*, *66*(12), 1476–1481. https://doi.org/10.1001/archneurol.2009.272

Styner, M., Oguz, I., Xu, S., Brechbühler, C., Pantazis, D., Levitt, J. J., … Gerig, G. (2006). Framework for the statistical shape analysis of brain structures using SPHARM-PDM. *Insight Journal*, *1071*, 242–250 Retrieved from http://www.pubmedcentral.nih.gov/articlerender.fcgi?artid=3062073&tool=pmcentrez&rendertype=abstract

Sullivan, M. D., Anderson, J. A. E., Turner, G. R., & Spreng, R. N. (2019). Intrinsic neurocognitive network connectivity differences between normal aging and mild cognitive impairment are associated with cognitive status and age. *Neurobiology of Aging*, *73*, 219–228.

Thambisetty, M., Wan, J., Carass, A., An, Y., Prince, J. L., & Resnick, S. M. (2010). Longitudinal changes in cortical thickness associated with normal aging. *NeuroImage*, *52*(4), 1215–1223. https://doi.org/10.1016/j.neuroimage.2010.04.258

Tomasi, D., & Volkow, N. D. (2012). Aging and functional brain networks. *Molecular Psychiatry*, *17*(5), 549–558. https://doi.org/10.1038/mp.2011.81

Tromp, D., Dufour, A., Lithfous, S., Pebayle, T., & Després, O. (2015). Episodic memory in normal aging and Alzheimer disease: Insights from imaging and behavioral studies. *Ageing Research Reviews*, *24*, 232–262. https://doi.org/10.1016/j.arr.2015.08.006

Turner, M. L., & Engle, R. W. (1989). Is working memory capacity task dependant? *Journal of Memory and Language*, *28*(2), 127–154.

van den Heuvel, M. P., & Sporns, O. (2013). Network hubs in the human brain. *Trends in Cognitive Sciences*, *17*(12), 683–696. https://doi.org/10.1016/j.tics.2013.09.012

Van Essen, D. C., Ugurbil, K., Auerbach, E., Barch, D., Behrens, T. E. J., Bucholz, R., … Yacoub, E. (2012). The Human Connectome Project: A data acquisition perspective. *NeuroImage*, *62*(4), 2222–2231. https://doi.org/10.1016/j.neuroimage.2012.02.018

Van Petten, C. (2004). Relationship between hippocampal volume and memory ability in healthy individuals across the lifespan: Review and meta-analysis. *Neuropsychologia*, *42*, 1394–1413.

Van Rooden, S., Van Den Berg-Huysmans, A. A., Croll, P. H., Labadie, G., Hayes, J. M., Viviano, R., … Damoiseaux, J. S. (2018). Subjective cognitive decline is associated with greater white matter hyperintensity volume. *Journal of Alzheimer's Disease*, *66*(3), 1283–1294. https://doi.org/10.3233/JAD-180285

Vandenberghe, R., Van Laere, K., Ivanoiu, A., Salmon, E., Bastin, C., Triau, E., … Brooks, D. J. (2010). 18F-flutemetamol amyloid imaging in Alzheimer disease and mild cognitive impairment a phase 2 trial. *Annals of Neurology*, *68*(3), 319–329. https://doi.org/10.1002/ana.22068

Verfaillie, S. C. J., Pichet Binette, A., Vachon-Presseau, E., Tabrizi, S., Savard, M., Bellec, P., … Yu, E. (2018). Subjective cognitive decline is associated with altered default mode network connectivity in individuals with a family history of Alzheimer's disease. *Biological Psychiatry: Cognitive Neuroscience and Neuroimaging*, *3*(5), 463–472. https://doi.org/10.1016/j.bpsc.2017.11.012

Viviano, R. P., Hayes, J. M., Pruitt, P. J., Fernandez, Z. J., van Rooden, S., van der Grond, J., … Damoiseaux, J. S. (2019). Aberrant memory system connectivity and working memory performance in subjective cognitive decline. *NeuroImage*, *185*, 556–564. https://doi.org/10.1016/j.neuroimage.2018.10.015

Vos de Wael, R., Larivière, S., Caldairou, B., Hong, S.-J., Margulies, D. S., Jefferies, E., … Bernhardt, B. C. (2018). Anatomical and microstructural determinants of hippocampal subfield functional connectome embedding. *Proceedings of the National Academy of Sciences*, *115*(40), 10154–10159. https://doi.org/10.1073/pnas.1803667115

Walhovd, K. B., Fjell, A. M., Dale, A. M., Fischl, B., Quinn, B. T., Makris, N., … Reinvang, I. (2006). Regional cortical thickness matters in recall after months more than minutes. *NeuroImage*, *31*(3), 1343–1351. https://doi.org/10.1016/j.neuroimage.2006.01.011

Walhovd, K. B., Fjell, A. M., Reinvang, I., Lundervold, A., Fischl, B., Quinn, B. T., & Dale, A. M. (2004). Size does matter in the long run: Hippocampal and cortical volume predict recall across weeks. *Neurology*, *63*(7), 1193–1197. https://doi.org/10.1212/01.WNL.0000140489.33249.95

Wang, K., Liang, M., Wang, L., Tian, L., Zhang, X., Li, K., & Jiang, T. (2007). Altered functional connectivity in early Alzheimer's disease: A resting-state fMRI study. *Human Brain Mapping*, *28*(10), 967–978. https://doi.org/10.1002/hbm.20324

Wechsler, D. (2008). *Wechsler adult intelligence scale* (4th ed.). San Antonio, TX: NCS Pearson Vol. 22.

Wilson, R. S., Boyle, P. A., Segawa, E., Yu, L., Begeny, C. T., Anagnos, S. E., & Bennett, D. A. (2013). The influence of cognitive decline on well-being in old age. *Psychology and Aging*, *28*(2), 304–313. https://doi.org/10.1037/a0031196

Wisdom, N. M., Callahan, J. L., & Hawkins, K. A. (2011). The effects of apolipoprotein E on non-impaired cognitive functioning: A meta-analysis. *Neurobiology of Aging*, *32*(1), 63–74. https://doi.org/10.1016/j.neurobiolaging.2009.02.003

Wold, H. (1966). Estimation of principal components and related models by iterative least squares. In *Multivariate Analysis* (pp. 391–420). New York: Academic Press.

Worsley, K., Taylor, J., Carbonell, F., Chung, M., Duerden, E., Bernhardt, B., … Evans, A. (2009). SurfStat: A Matlab toolbox for the statistical analysis of univariate and multivariate surface and volumetric data using linear mixed effects models and random field theory. *NeuroImage*, *47*, S102. https://doi.org/10.1016/S1053-8119(09)70882-1

Yang, Z., Wen, W., Jiang, J., Crawford, J. D., Reppermund, S., Levitan, C., … Sachdev, P. S. (2016). Age-associated differences on structural brain MRI in nondemented individuals from 71 to 103 years. *Neurobiology of Aging*, *40*, 86–97. https://doi.org/10.1016/j.neurobiolaging.2016.01.006

Yao, Z., Hu, B., Liang, C., Zhao, L., & Jackson, M. (2012). A longitudinal study of atrophy in amnestic mild cognitive impairment and Normal aging revealed by cortical thickness. *PLoS One*, *7*(11), e48973. https://doi.org/10.1371/journal.pone.0048973

Yeo, B. T., Krienen, F. M., Sepulcre, J., Sabuncu, M. R., Lashkari, D., Hollinshead, M., … Buckner, R. L. (2011). The organization of the human cerebral cortex estimated by functional connectivity. *Journal of Neurophysiology*, *3*(6), 1125–1165. https://doi.org/10.1152/jn.00338.2011

Yonelinas, A. P., Widaman, K., Mungas, D., Reed, B., Weiner, M. W., & Chui, H. C. (2007). Memory in the aging brain: Doubly dissociating the contribution of the hippocampus and entorhinal cortex. *Hippocampus*, *17*(11), 1134–1140. https://doi.org/10.1002/hipo.20341

Zachary, R. A. (1986). *Shipley Institute of Living Scale: Revised manual*. Los Angeles: Eastern Psychological Services.

Zeighami, Y., Fereshtehnejad, S. M., Dadar, M., Collins, D. L., Postuma, R. B., Mišić, B., & Dagher, A. (2017). A clinical-anatomical signature of Parkinson's disease identified with partial least squares and magnetic resonance imaging. *NeuroImage*, *190*, 69–78. https://doi.org/10.1016/j.neuroimage.2017.12.050

Zhang, Y., Brady, M., & Smith, S. (2001). Segmentation of brain MR images through a hidden Markov random field model and the expectation-maximization algorithm. *IEEE Transactions on Medical Imaging*, *20*(1), 45–57. https://doi.org/10.1109/42.906424

Zhao, T., Cao, M., Niu, H., Zuo, X. N., Evans, A., He, Y., … Shu, N. (2015). Age-related changes in the topological organization of the white matter structural connectome across the human lifespan. *Human Brain Mapping*, *36*(10), 3777–3792. https://doi.org/10.1002/hbm.22877

Zhao, X., Lynch, J. G., & Chen, Q. (2010). Reconsidering Baron and Kenny: Myths and truths about mediation analysis. *Journal of Consumer Research*, *37*(2), 197–206. https://doi.org/10.1086/651257

Ziegler, D. A., Piguet, O., Salat, D. H., Prince, K., Connally, E., & Corkin, S. (2010). Cognition in healthy aging is related to regional white matter

integrity, but not cortical thickness. *Neurobiology of Aging*, *31*(11), 1912–1926. https://doi.org/10.1016/j.neurobiolaging.2008.10.015

SUPPORTING INFORMATION

Additional supporting information may be found online in the Supporting Information section at the end of this article.

How to cite this article: Lowe AJ, Paquola C, Vos de Wael R, et al. Targeting age-related differences in brain and cognition with multimodal imaging and connectome topography profiling. *Hum Brain Mapp*. 2019;40:5213–5230. https://doi.org/10.1002/hbm.24767